Transmission of JPEG2000 Images over Cognitive Radio Networks

by

Golara Javadi

B.Sc., Isfahan University of Technology, 2013

Thesis Submitted in Partial Fulfillment of the
Requirements for the Degree of
Master of Applied Science

in the
School of Engineering Science
Faculty of Applied Sciences

SIMON FRASER UNIVERSITY

Summer 2016

Approval

Name:	**Golara Javadi**
Degree:	**Master of Applied Science (Engineering Science)**
Title:	***Transmission of JPEG2000 Images over Cognitive Radio Networks***
Examining Committee:	**Chair:** Dr. Ash Parameswaran

Dr. Jie Liang
Senior Supervisor
Professor

Dr. Atousa Hajshirmohammadi
Co-Supervisor
Senior Lecturer

Dr. Paul Ho
Internal Examiner
Professor

Date Defended: August 12, 2016

Abstract

Cognitive Radio (CR) is an efficient way of spectrum utilization, because secondary users (SUs) with bandwidth-demanding applications such as multimedia can get access to licensed frequency resources opportunistically and resolve their bandwidth limitations. Among all multimedia formats, JPEG2000 is a suitable candidate for cognitive radio networks thanks to its unique features. In conventional resource allocations for CR systems, all data bits are assumed equally important. However, different parts of the JPEG2000 bit stream have different contributions to the quality of the received image. Therefore, in this paper, an unequal power allocation method is used to allocate the available power to the coded bits based on their importance in the image quality. Furthermore, bits with higher significance are further protected by using sub-channels with better channel quality. Thus, the likelihood of significant bits being received correctly is increased. The optimal solution is obtained by minimizing the image distortion without violating the interference requirement of the primary users (PU). The performance of the proposed method is demonstrated by simulation results.

Keywords: Cognitive Radio; OFDM; Multimedia; JPEG2000; Resource allocation; Unequal power allocation; Multipath/ Fading channels

Dedication

To my beloved parents, my dear brother, my lovely sister and my love Mehdi

Acknowledgements

First and foremost, I would like to sincerely thank my two remarkable supervisors, Dr. Jie Liang and Dr. Atousa Hajshirmohammadi, for their everlasting care and support. It indeed is a great opportunity to be surrounded by advisors who have tremendous knowledge, experience, motivation, and insight; I was honoured to experience that and will remain to do so.

My sincere thanks also goes to Dr. Paul Ho and and Dr. Rodney G. Vaughan for their keen comments and encouragement, which inspired me to widen my research from various perspectives. Throughout this degree, I have been enrolled in several informative courses that were taught by Dr. Greg Mori, Dr. Rodney G. Vaughan, and audited Dr. Paul Ho's course; I sincerely appreciate such an exemplary dedication and comprehensive sessions.

I would like to thank my colleague, namely Moein Shayegannia for the short yet enjoyable collaborative experience. I would also like to thank my colleagues, lab mates, and friends for the good times spent together. I am very grateful for the faculty and staff of the School of Engineering Science and graduate student society for their support and help.

Lastly, I would like to say that no matter how many times I thank my beloved family, it would not be sufficient. Their patience, compassion, and advices is what urges me to better myself.

Table of Contents

List of Tables

List of Figures

List of Acronyms

AWGN	Additive White Gaussian Noise
BER	Bit Error Rate
BPC	Bit Plane Coding
CB	Coding Blocks
CIR	Channel Impulse Response
CP	Coding Pass
CR	Cognitive Radio
CSI	Channel State Information
DARPA	Defense Advanced Research Projects Agency
DFT	Discrete Fourier Transform
DVC	Distributed Video Coding
DWT	Discrete Wavelet Transform
EBCOT	Embedded Block Coding with Optimized Truncation
EPA	Equal Power Allocation
FCC	Federal Communication Commission
ICT	Irreversible Color Transform
IFFT	Inverse Fast Fourier Transform
ISI	Inter-Symbol Interference
ISO	International Organization for Standardization
ITU	International Telecommunication Union
JPEG	Joint Photographic Expert Group
MSE	Mean Square Error
OFDM	Orthogonal Frequency Division Multiplexing
OFDMA	Orthogonal Frequency Division Multiplexing Access
PAPR	Peak to Average Power Ratio
PSD	Power Spectral Density
PSNR	Peak Signal to Noise Ratio
QoS	Quality of Service
RCT	Reversible Color Transform
SA	Simulated Annealing

SNR	Signal to Noise Ratio
SPTF	Spectrum Policy Task Force
UPA	Unequal Power Allocation
UWB	Ultra-Wide Band

List of Symbols

$E\{\}$	Expected value
$(.)^T$	Transposition
$\|.\|$	Absolute value
$sign(.)$	Sign function
$(.)^H$	Complex conjugate transpose operation
$\forall$	For all, For any
$*$	Convolution operator
$Q(.)$	Q function

Chapter 1.

Introduction

1.1. Motivation

The rapid developments in technology have made all types of applications available in a single mobile handset and the most popular ones are multimedia applications. The growing demand in wireless image and video transmission requires high data rate and reliable transmission of multimedia stream over severe channel conditions. However, the radio frequency spectrum, which is a natural resource, is finite. Therefore, the cellular wireless services can only utilize the quota which is allocated to them by regulatory agencies. Although the wireless access requests by cellular service providers is expected to increase continuously in the course of time, the competing interests and fundamental physical laws, restrict the RF bandwidth allocation growth [1]. The exponential demand for wireless “bandwidth” coupled with the very limited supply of RF bandwidth impose challenges in maintaining high quality received videos and images. Furthermore, since the power of base station is limited due to cost and radiation constraints, power efficiency, in addition to spectral efficiency, is crucial.

Underutilization of the licensed frequency spectrum [2], is an incentive to look for feasible spectrally-efficient designs. Utilization of the primary spectrum varies from 15% to 85%, according to the US Federal Communication Commission (FCC) [3,4]. Based on another study, which was conducted in major US cities, large portions of the spectrum below 1 GHz was not being used for significant periods of time [2]. One of the main reasons for the notable underutilization of the allocated spectrum is the fixed spectrum

policy under which the operator leases a spectrum for fixed and relatively long periods of time (several years). Therefore, a Spectrum Policy Task Force (SPTF) is devised to modify the spectrum allocation policies, so that the idle spectrum can be avoided at any given time and location. Following this policy, several organizations such as the US Defense Advanced Research Projects Agency (DARPA), the IEEE 802.22 Working Group and MITRE Corporation has started development of standards and technologies for dynamic access and sharing of spectrum [2]. Cognitive ratio (CR) networks help facilitate this initiative significantly. Cognitive radio has emerged as a powerful platform for unlicensed devices to use licensed bands under certain conditions and the platform was approved by FCC [3] to increase the spectrum usage efficiency. Coexistence of primary user and secondary user requires some flexibilities in the spectrum shape of the transmitted signals. Orthogonal Frequency Division Multiplexing (OFDM) offers this kind of flexibilities by filling the spectral gaps without interfering with primary users [4]. However, a major problem with this kind of applications is the mutual interference between primary and secondary users, which is taken into account in this thesis.

Multimedia transmission is a suitable candidate to be benefitted from cognitive radio technology, because of its bandwidth demands and rigorous delay constraints. In this thesis, we focus on the transmission of scalable images over wireless channels. Scalable bit-streams are more sensitive to channel errors caused by fading and interference. A single bit error in the encoded image can cause error propagation, which affects large areas of the image, resulting in image quality degradations. Therefore, reducing the amount of bits required for representing the image, leads to less image quality degradation.Hence, selecting an efficient source coder for reducing the number of required bits is another objective of this work. Note that having smaller amount of bits reduces the required bandwidth to transmit data. JPEG2000 standard provides high compression efficiency and has unique features, which will be described later in this thesis. These features make JPEG2000 a very appealing candidate for wireless multimedia applications over cognitive radio. The JPEG2000 coded bit-stream has a hierarchical structure, in which some bits hold more important information compared to others, thus higher protection over the more important bits is rational to achieve a higher quality through image transmission in an error prone wireless channel.

Most of the previously performed researches with the focus on CR networks, considered maximizing the throughput of the secondary users as one of the most important design criteria. Thus, other quality measures for the secondary users, such as distortion for multimedia applications, are ignored in most occasions. However, recent investigation by Jian et. al. in [5] reveals that maximizing throughput does not necessarily enhance Quality of Service (QoS) at the application layer for some multimedia applications.

The main objective of this research is to investigate an optimized resource allocation technique to facilitate multimedia bit-stream transmission over OFDM-based CR networks to overcome the frequency selectivity of the wireless channel and fulfill the interference restrictions on licensed users. This is achieved by maximizing the quality of the receiving image subject to interference and power constraints. Two important quality metrics are used in this regards that are: i) received image Peak Signal-to-Noise Ratio (PSNR), and ii) Bit Error Rate (BER).

1.2. Thesis Contributions

In this thesis, the problem of improving the quality of transmitted JPEG2000 images over the secondary channel in cognitive radio networks is studied. Some features of the proposed scheme are as the followings [6]:

- To achieve higher bandwidth efficiency and lower system complexity, which are essential factors in transmission over CR, the inherent scalable properties of the JPEG2000 bit-stream along with Unequal Power Allocation (UPA) is utilized to protect the important bits.

- In contrast to the previously published works [7]–[9] that used channel availability to make the secondary user access decision, in this thesis, Channel State Information (CSI) (channel gain) is used by secondary users to help make the optimal decision for maximizing the QoS.

- To avoid exceeding the primay user's tolerance of collision level, which is dependent on the primary service type, an interference constraint is considered in the resource allocation problem. Necessary power adjustments based on CSI are done prior to transmission to prevent primary user transmission quality degradation.

- To maintain the overall transmit reliability, an adaptive modulation is adopted. Based on the number of available sub-channels to transmit the data, different modulations are mapped to keep a constant throughput. As the number of available sub-channels decrease due to primary user appearance or interference constraint, the modulation level increases.

1.2.1. Scholarly Publications

The contribution of this thesis resulted in publications listed below.

- G. Javadi, A. Hajshirmohammadi, and J. Liang, "JPEG2000 Image Transmission Over OFDM-Based Cognitive Radio Network," in IEEE Computing and Communication Conference (IEMCON), Vancouver, 2015.

- G. Javadi, A. Hajshirmohammadi, and J. Liang, "Power and Sub-channel Optimization of JPEG2000 Image Transmission over OFDM-Based Cognitive Radio Networks" to be submitted to IET Communications.

1.3. Thesis Structure

Chapter 2 presents the thesis background, and summarizes the pertinent literature in the field of cognitive radio networks and transmission of multimedia streams

in them. Chapter 3 describes an algorithm of sub-channel allocation for transmission of JPEG2000 codec over OFDM based cognitive radio. Our proposed power and sub-channel allocation method is illustrated in Chapter 4. Finally, Chapter 5 summarizes the conclusion of this thesis and provides further work directions.

Chapter 2.

Background and Related Works

This chapter provides a brief overview of the key concepts related to the thesis, such as cognitive radio and in particular dynamic spectrum sharing in secondary networks, OFDM application in cognitive radio, JPEG2000 image coder structure, and introduces some of the protection techniques in the literature for image transmission over wireless channels. Related investigations that are performed in the field of cognitive radio networks are also summarized in this chapter.

2.1. Background

2.1.1. Cognitive Radio Networks

In recent years, the enormous increase in the wireless networks and the devices operating in these networks has led to spectrum scarcity. The measurements showed that many parts of the spectrum can be used more efficiently. Further studies have shown that the main cause of spectrum scarcity is the licensing process. Therefore, some parts of the frequency is allocated to the services that they never use, also unbalance allocation due to miss-prediction of the demand is another cause of scarcity. In general, getting access to the spectrum resources for the new users and services is difficult in this policy.

This fact necessitates a new communication paradigm to use the radio frequency band in a more efficient way. Several methods were developed in the literature to access

the licensed bands as a secondary user. Ultra-Wide Band (UWB) transmission and Cognitive Radio are two instances of these methods.

Cognitive Radio, first introduced by Mitola in [10] as a solution to address the shortage of available radio spectrum. A more rigorous definition of CR is provided by Haykin [11] as follows.

"Cognitive radio is an intelligent wireless communication system that is aware of its surrounding environment (i.e., outside world), and uses the methodology of understanding-by-building to learn from the environment and adapt its internal states to statistical variations in the incoming RF stimuli by making corresponding changes in certain operating parameters (e.g., transmit power, carrier frequency, and modulation strategy) in real-time, with two primary objectives in mind:

- Highly reliable communications whenever and wherever needed;
- Efficient utilization of the radio spectrum."

Parameter adaptation can be based on several factors such as radio spectrum availability, channel bandwidth and gain, primary user behavior, and QoS requirements. To build highly reliable communication, a secondary user must limit interference with primary users.

Architecture

Cognitive radio architecture consists of three main components: primary network, secondary network, and shared channel. In primary network users have exclusive access to licensed spectrum bands. Primary network consists of: (i) primary users and (ii) primary base station. Secondary network is not licensed to operate in a certain frequency band, but can access the licensed band of primary users in an opportunistic or negotiated manner. The components of a secondary network are: (i) secondary users, (ii) secondary base station and (iii) spectrum broker, a scheduling server that shares the

spectrum resources between different cognitive radio networks. The licensed spectrum is a shared resource between primary and secondary.

The most important issue in licensed band operations among secondary users is avoiding interference with primary users. This is done through spectrum hand-off, which means that in the presence of any other primary user, secondary users shall vacate the spectrum band immediately and move to the next available band. In licensed band operations, all the secondary users have the same right to access the unlicensed spectrum which necessitates the use of intelligent spectrum sharing algorithms.

In conclusion, secondary users are required to continually check the existence of primary user in a cycle consist of four main functionalities, which can be listed as follows [3]:

1. **Spectrum sensing:** The ability to sense the spectrum at any time and location, in order to determine which portions of the spectrum are available.

2. **Spectrum management:** The ability to allocate the best available spectrum band based on the availability of the spectrum and other policies.

3. **Spectrum mobility:** The ability to vacate the spectrum in the presence of any primary user and move to the next best available spectrum band

4. **Spectrum sharing:** The ability to provide a fair and optimal spectrum allocation method among multiple secondary users.

Dynamic spectrum sharing

Different dynamic spectrum access strategies are available in the literature [12], which can broadly categorize under three models:

- Dynamic exclusive use model
- Open sharing model
- Hierarchical access model

Our focus in this thesis is on the last method, i.e., hierarchical access model. In the hierarchical access model, secondary users are allowed to use the licensed spectrum under the condition that implies the secondary users cannot interfere with primary users beyond a certain probability of collision or interference level. Two strategies that authorize the simultaneous existence of primary and secondary users are spectrum underlay and overlay. When the transmission power of secondary users is confined to the noise floor of primary users, spectrum underlay approach has been utilized (e.g., UWB), and when the restrictions on secondary users are imposed on where and when they can transmit, an overlay scheme has been implemented. (Figure 1).

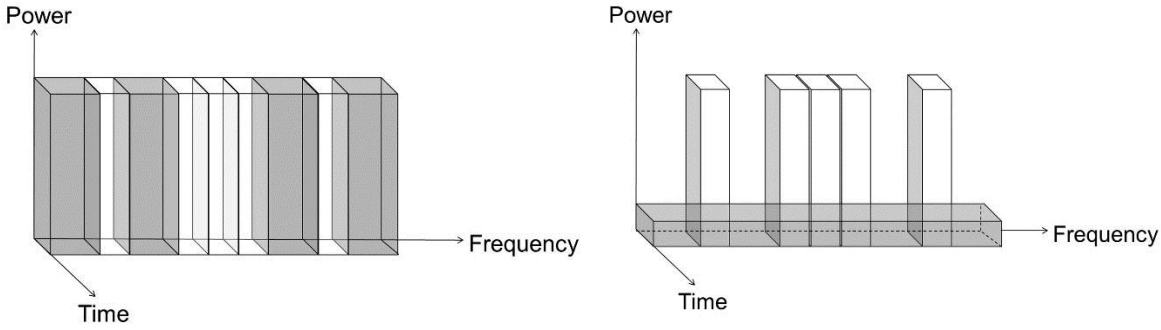

(a) (b)

Figure 1. (a) Spectrum overlay (b) Spectrum underlay

Our proposed scheme falls in the spectrum overlay hierarchical access model classification. The hierarchical access model is the most compatible approach with the current spectrum management policies, and provides better spectrum efficiency in the licensed bands.

Opportunity Exploitation

Once spectrum opportunities have been identified, a secondary user must determine how to exploit them. Moreover, opportunities may not present themselves over contiguous frequency bands. Thus, an access strategy with flexibility in the spectrum shape of transmitting signal is required. OFDM offers this flexibilities by filling

the spectral gaps without interfering with primary users [4]. The subcarrier structure of OFDM can be configured for efficient usage of spectral holes, because if the primary user appears in any subcarrier the transmission can continue on other OFDM subcarriers.

OFDM has many other advantages that makes it suitable for CR networks. High data rate transmission is feasible in OFDM by multi-carrier modulation. Moreover, it improves the frequency selectivity of the wideband channel experience by single-carrier transmission. Supporting higher data rate in a single carrier transmission requires wider bandwidth. As the symbol rate becomes larger than the coherence bandwidth of the wireless channel, the link suffers from multipath fading and experiences the inter-symbol interference (ISI). To handlethe resultant ISI from the time-varying multi-path fading channel, adaptive equalizers are employed. The complexity of an equalizer increases with the data rate. Transmission of a high data rate single-carrier may not be feasible due to excessive complexity of the equalizer in the receiver [13]. The general idea of multi-carrie modulation is to divide the transmitted bit stream into a number of different sub-streams and send them over various sub-channels. As a result, data rate of each sub-channel is less than the total data rate, and the corresponding sub-channel bandwidth is much less than the total system bandwidth. Usually, the sub-channels are orthogonal to each other and the number of sub-streams are chosen such that it ensures two factors: i) sub-channel bandwidth is less than the coherence bandwidth of the channel and therefore, each sub-channel experiences flat fading; ii) reduces the resulted ISI as much as possible. This is shown in Figure 2. Multicarrier modulation is efficiently implemented digitally in OFDM. In this discrete implementation the ISI can be completely eliminated through the use of a cyclic prefix. Note that the frequency-nonselectivity of narrowband channels reduces the complexity of the equalizer [14].

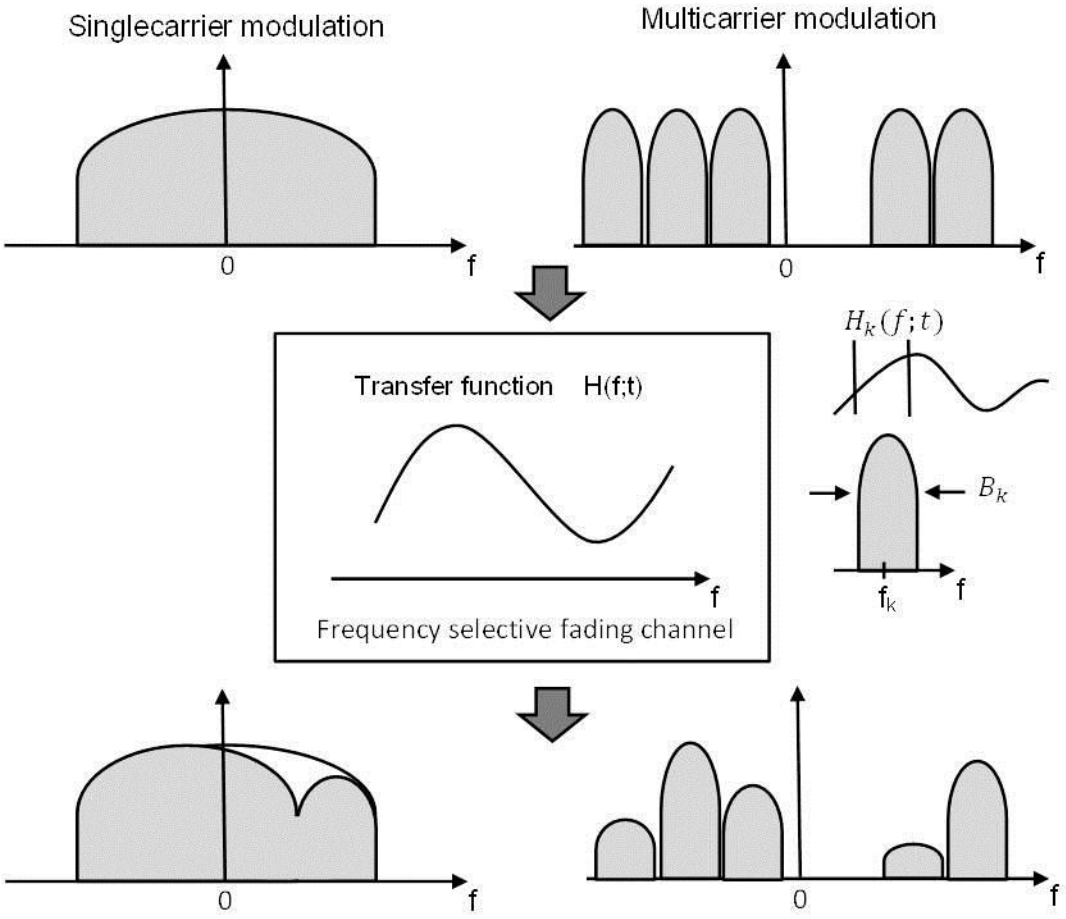

Figure 2. Multichannel transmission Vs. single channel transmission

To ensure nonintrusive communication with primary users, any spectral leakage as well as the nonlinearity of the transmitter power amplifier should be controlled. Additionally, the impact of nulled subcarriers on the Peak-to-Average-Power Ratio (PAPR) of the transmitted OFDM signal requires careful study.

2.1.2. JPEG2000 Standard

As illustrated in Table 1, images require large storage space, transmission bandwidth, and long transmission time. That gives the motivation for the image compression. With the current state of technology, the only solution is to compress images before storage and transmission.

Table 1. Storage and transmission needs of various types of uncompressed images [15]

Image Type	Size	Bits/Pixel	Uncompressed Size	Transmission Bandwidth	Transmission Time (using a 28.8K modem)
Grayscale	512×512	8 bpp	262 Kbytes	2.1 Mbit/image	1 min 13 sec
Color	512×512	24 bpp	786 Kbytes	6.29 Mbit/image	3 min 39 sec
Medical	2048×2048	12 bpp	5.16 Mbytes	41.3 Mbit/image	23 min 54 sec
Super High Density (SHD)	2048×2048	24 bpp	12.58 Mbytes	100 Mbit/image	58 min 15 sec

Starting the mid-1980s, members from both the International Telecommunication Union (ITU) and the International Organization for Standardization (ISO) have been working together to establish a joint international standard for the compression of grayscale and color still images. This effort has been known as the Joint Photographic Experts Group (JPEG), where the “joint” in JPEG refers to the collaboration between ITU and ISO. The JPEG2000 international standard represents advances in image compression technology where the image coding system is optimized for efficiency, scalability and interoperability in network and mobile environments to fulfill today’s digital imagery requirements. The JPEG2000 standard provides a set of features to serve the market and applications better in terms of addressing the areas where previous standards failed to perform and produce the best quality [16]. The JPEG2000 standard is used in wide application areas such as Internet, digital photography, digital library, image archival, compound documents, image databases, color reprography (photocopying, printing, scanning, facsimile), graphics, medical imaging, multispectral imaging such as remotely sensed imagery, satellite imagery, mobile multimedia communication, client-

server networking, e-commerce, etc. This section provides a brief understanding of the JPEG2000 structure and discusses the major features of this standard.

Structure

The general block diagram of the JPEG2000 encoder and decoder is illustrated in Figure 3. The encoder side can be divided into three phases: (i) image preprocessing, (ii) compression, and (iii) compressed bit-stream formation.

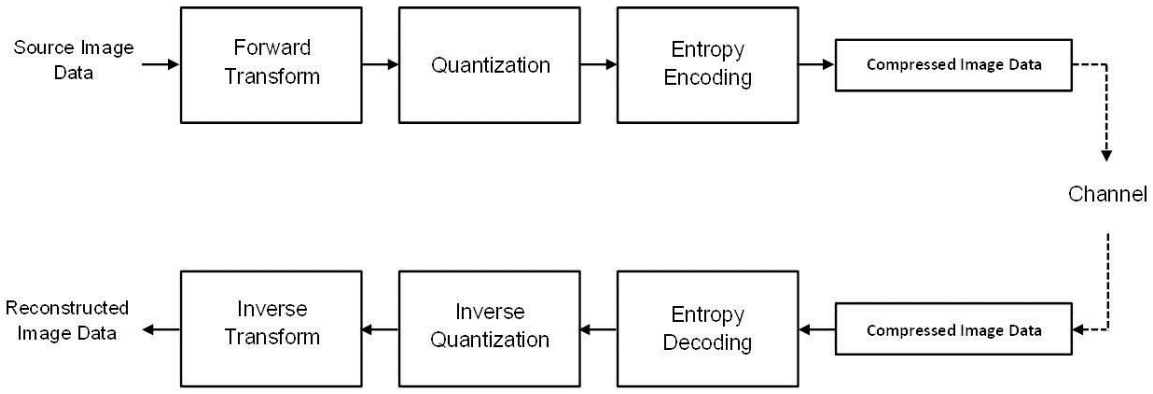

Figure 3. General block diagram of the JPEG2000 encoder and decoder

Image Preprocessing

Preprocessing functions are optional. The first preprocessing operation is tiling. If the raw image is very large, usually it is partitioned into a number of rectangular nonoverlapping blocks. Each of these blocks is called a tile. All the tiles have the same dimension except when the image dimension is not an integer multiple of the tile dimension. In that case, the tiles at the image boundary have different dimension. The tiles are compressed independently. Therefore, heavy quantization for very low bitrate compression may cause visible artifacts at the tile boundaries as it is typical in any block transform coding. Smaller tiles create more boundary artifacts and also degrade the compression efficiency compared to larger ones. It is worth mentioning that no tiling offers the best visual quality. However, large tile size requires large memory buffers for

implementation. Typical tile size based on the cost, area, and power compaction is 256×256 or 512×512.

After that, other preprocessing functions that can be applied are DC level shifting and multicomponent transformation. The purpose of applying a DC level shifting is to ensure that the input image samples have approximately a dynamic range centered around the zero. The multicomponent transform is effective in reducing the correlations among the multiple components in a multicomponent image. This results in reduction of redundancy and increase the compression performance. Components can be interpreted as three color plane (R, G, B). However, they do not necessarily represent Red-Green-Blue data of a color image. That is why they are often called multicomponent color transmission as well. The JPEG2000 standard support both Reversible Color Transform (RCT) for lossless compression of an image and Irreversible Color Transform (ICT) for lossy compression.

Compression

After optional preprocessing phase the compression phase generates the compressed code with mainly three sequential steps: (i) Discrete Wavelet Transform (DWT) (ii) Quantization, and (iii) Entropy Encoding. The data flow of the compression system is shown in Figure 4. As shown in Figure 4, each preprocessed component is independently compressed and transmitted as shown in Figure 3.

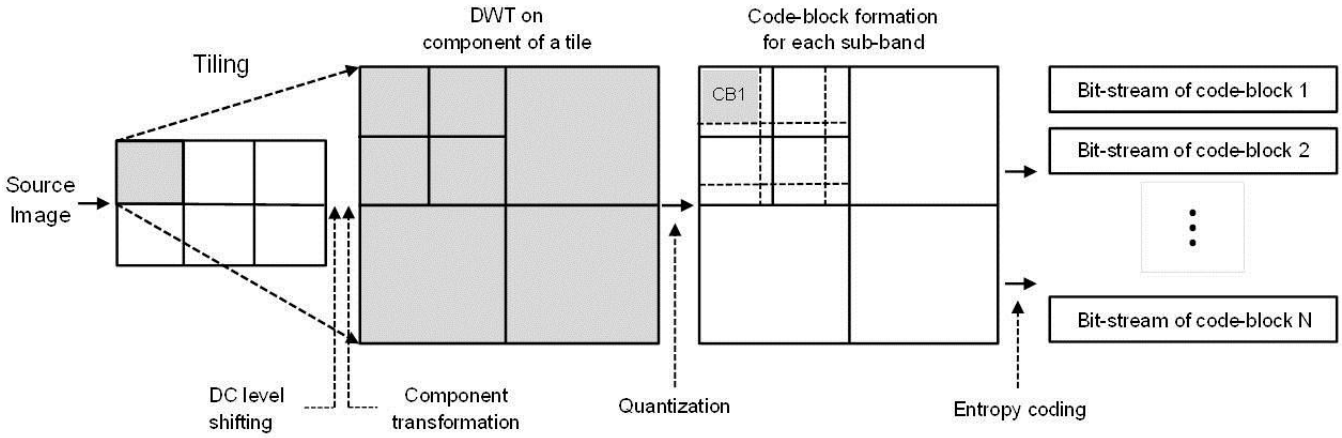

Figure 4. Data flow of JPEG2000 compression system

Each tile component is analyzed by a suitable DWT to decompose it into a number of sub-bands at different resolution levels. The two-dimensional DWT is performed by applying the one-dimensional DWT row-wise and then column-wise on each component as shown in Figure 5.

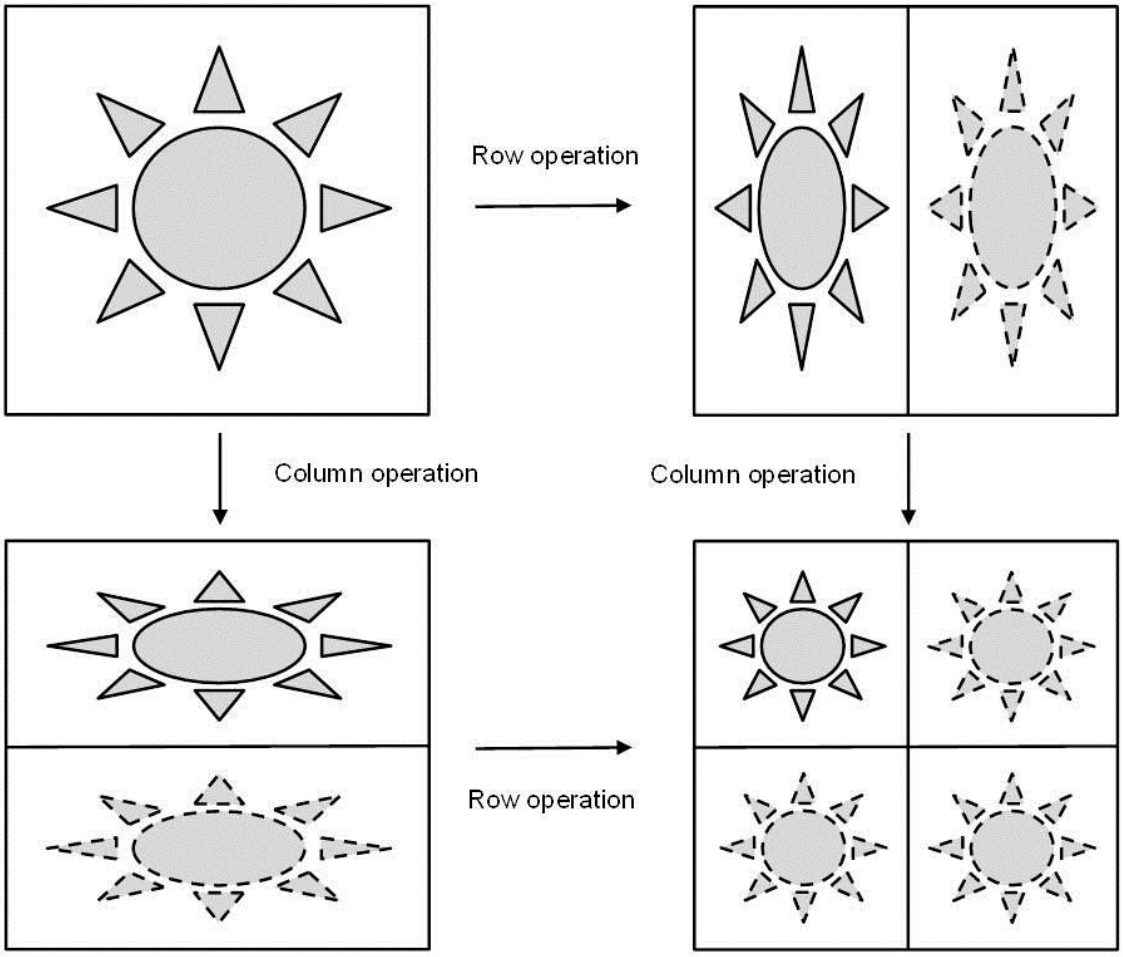

Figure 5. Extension of DWT in two-dimensional signals

Decomposition starts with creating four sub-bands LL1, HL1, LH1, and HH1. LL1, which is the low-pass sub-band, represents a 2:1 subsampled in both vertical and horizontal directions; therefore, it is a low-resolution version of the original component. The other sub-bands (HL1, LH1, HH1) represent a downsampled residual version of the original image needed for the perfect reconstruction of the original image. LL2, HL2, LH2, and HH2, can be produced by analyzing the LL1 sub-band once again. Similarly, higher levels of decomposition can be generated. Practically, no more compression can be achieved after five levels of decomposition in natural images. However, theoretically it can go even further. (Figure 6)

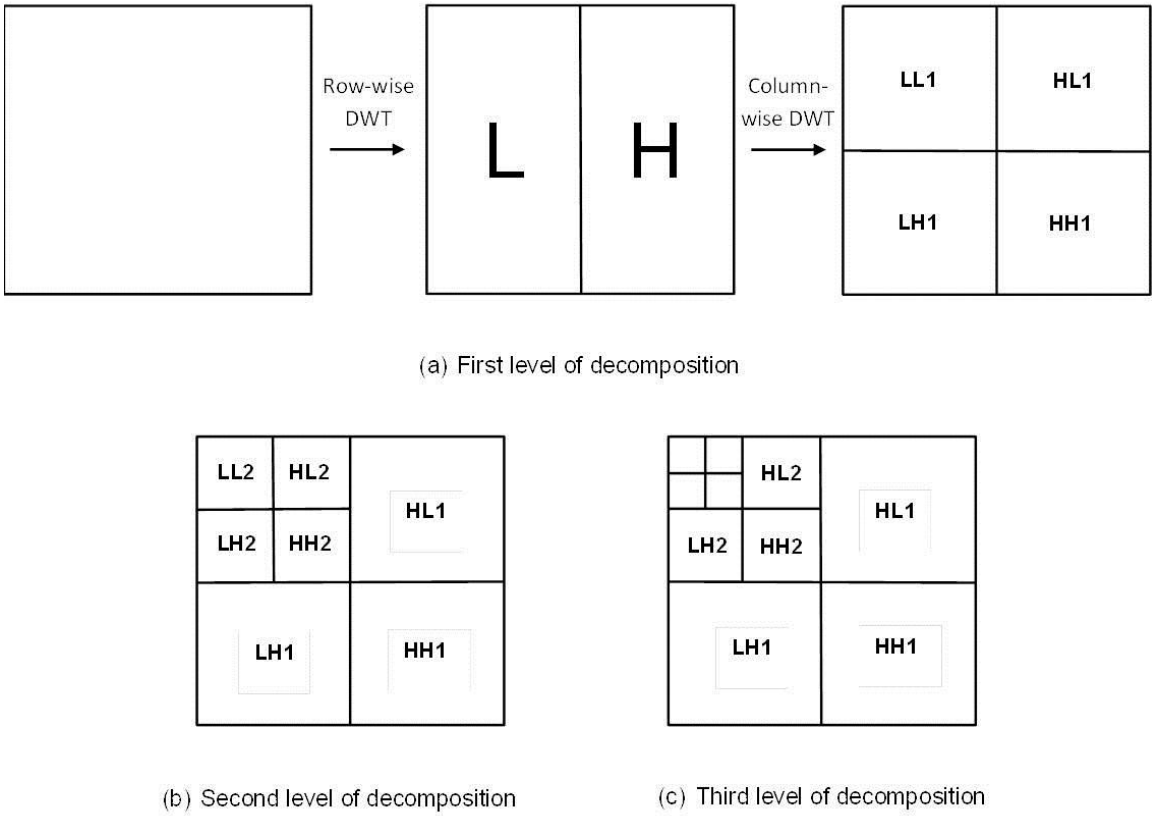

Figure 6. Row-Column computation of two-dimensional DWT

In order to reduce the precision of the sub-bands to aid in achieving compression after the DWT, all the sub-bands are quantized in lossy compression mode. One of the main sources of information loss in the encoder is the quantization of DWT sub-bands. In case of lossless encoding, quantization is not used. Different quantization step size for each sub-band is supported by the standard, which is calculated based on the dynamic range of the sub-band values according to:

$$q = sign(y)\left\lfloor \frac{|y|}{\Delta_b} \right\rfloor \tag{1.1}$$

where *y* is the input to the quantizer, *sign(y)* denotes the sign of *y*, Δ_b is the step size, and *q* is the resulting quantizer index. The standard use uniform quantizer with

deadzone, which means that the quantization range about 0 is $2\Delta_b$ as in Figure 7. This ensures that more zeros result.

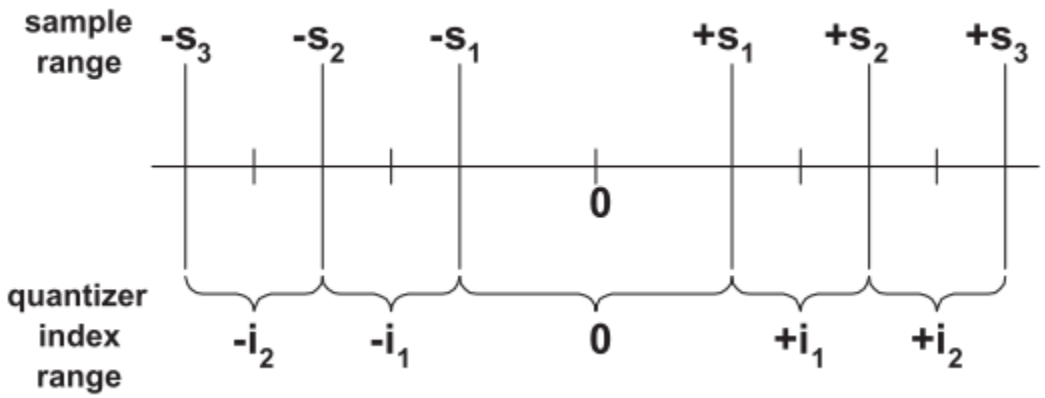

Figure 7. Deadzone quantizer structure

The quantized sub-bands are then divided into a number of smaller code-blocks of equal size as shown in Figure 7, except for the code-blocks at the boundary of each sub-band. The typical size of the code-blocks is usually 32 x 32 or 64 x 64 for better memory handling.

Physically the data are compressed by the entropy encoding of the quantized wavelet coefficients in each code-blocks. The code-blocks are encoded independently. Accordingly, the error propagation restricted to the code-block boundaries, that is, unsuccessful decoding of a code-block does not affect the decoding of the following code-blocks. Bits of equal significance across all the coefficients in a code block are referred to as a bit-plane. In JPEG2000 the Embedded Block Coding with Optimized Truncation (EBCOT) algorithm has been adopted for encoding each bit-plane in three coding passes with a part of bit-plane being coded in each coding pass. That is why the Bit-Plane Coding (BPC) is also called fractional bit-plane coding. These three coding passes are called the significant propagation pass, magnitude refinement pass, and cleanup pass. Each of the coding passes is applied to each bit-plane of a code-block except the first bit-plane (the most significant bit-plane), which is applied only with the cleanup pass. After each coding pass completes a run of scan pattern in the current bit-

plane, the next coding pass restarts the scan pattern from the beginning. These passes, collect contextual information, which is used for generating a separate compressed bit-stream for each code-block.

Bit-stream Formation

After the compressed bits for each code-block are generated, they are separated into packets. One packet is generated for each precinct in a tile. A precinct is essentially a grouping of code blocks within a resolution level. Since precincts cannot overlap code-blocks and must have dimensions that are exact powers of 2, the precinct size restricts the subordinate code-block partitions. An example of precinct partitioning is shown in Figure 8. [15]

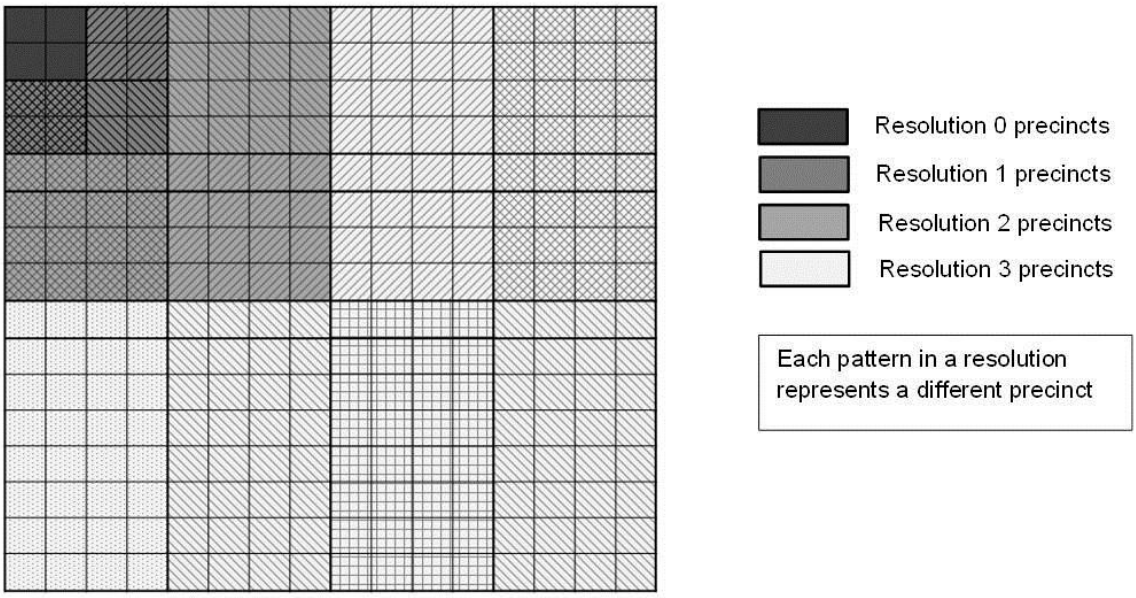

Figure 8. An example of precincts partitioning

Each packet comprises of a header and the compressed data. Then, the packets are multiplexed together in an ordered manner to form one code-stream. The organization of the code-stream can be seen in Figure 9. There are five built-in ways to order the packets, called progressions.

- **Quality:** layer, resolution, component, position

As more data are received, image quality is improved, by receiving the first few bytes of data, a low quality rendition of the image can be decoded and as more bytes are received, they can be combined with previously received bytes for progressively higher quality rendition.

- **Resolution 1:** resolution, layer, component, position

In this type the first few bytes are used to represent a small thumbnail of the image. With more bytes of data resolution or size of the image gets better.

- **Resolution 2:** resolution, position, component, layer

- **Position:** position, component, resolution, layer

The image will received from top to bottom and is useful for memory constrained applications such as printers.

- **Component:** component, position, resolution, layer

This type controls the order in which the data corresponding to different components is decoded, that is, the grayscale version of an image might first be decoded, followed by color information, followed by overlaid annotations, text, etc. JPEG2000 supports images with up to 16384 components. Commonly, images are 1 component (grayscale), 3 components (e.g., RGB, YUV, etc.), or 4 components (CMYK). Most images with more than 4 components are from scientific instruments.

The sorting mechanisms are ordered from most significant to least significant. For example, in the case of quality progression, packets are ordered first by layer, second by resolution, third by component, and fourth by position, where position refers to the precinct number [17].

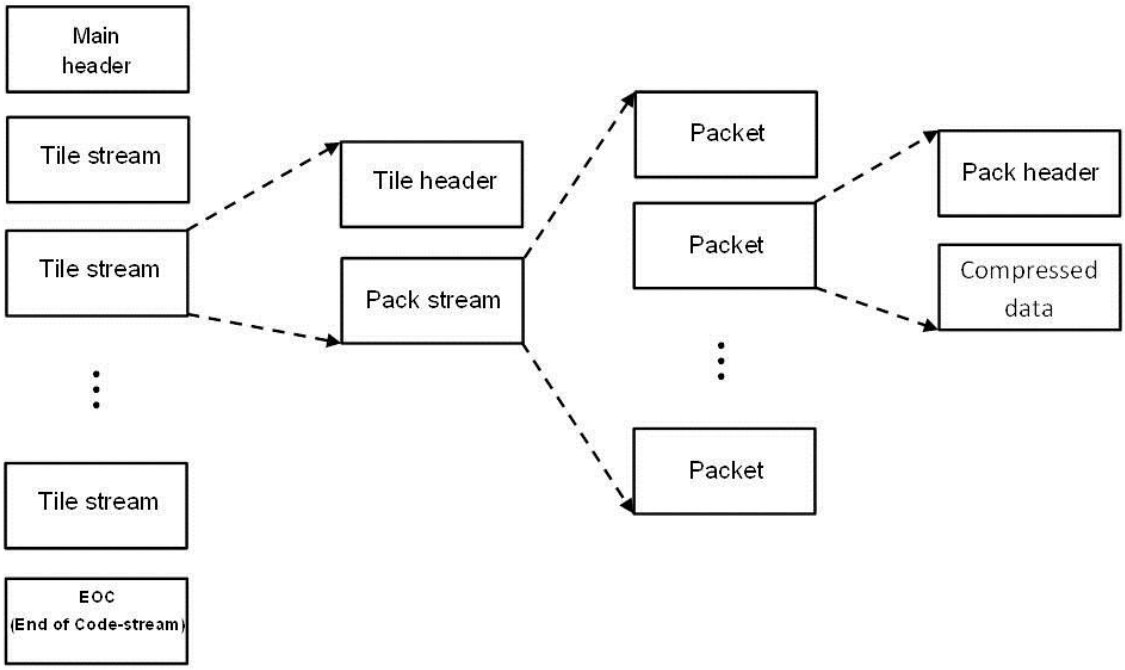

Figure 9. Code-stream organization [15]

In this work, quality progression is used in which the arrangement of bits are from the most to the least significant ones in the image quality. Bits are sorted by quality layer structure. Each layer consists of a number of consecutive bit-plane coding passes from each code-block in the tile, including all sub-bands of all components for that tile. The coding passes among all code-blocks are distributed across different layers subject to target bit rate constraint of each layer, as shown in Figure 10. The first layer generates a low quality version of the image and other layers enhance the decoded image quality. In other words, a layer could be interpreted as one quality increment for the entire full resolution image, and at any stage the image can be reconstructed by truncation of these layers.

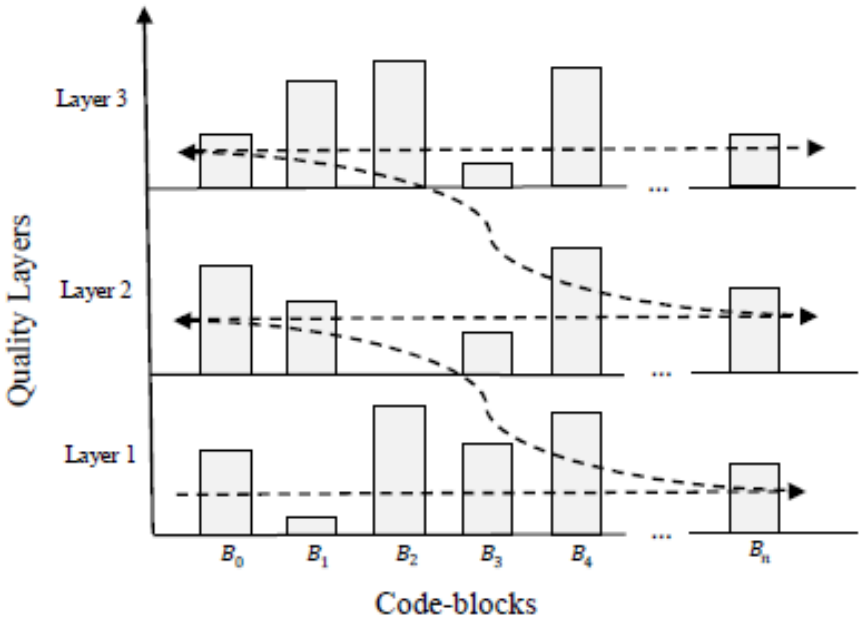

Figure 10. Code block contributions to quality layers, indicating a quality progressive pack-stream ordering

The final generated code stream has a main header at the beginning. The main header describes the original image information and the various settings that are used in the encoding process. This information enables the decoder to reconstruct the image with the desired characteristics.

The JPEG2000 Feature Set

The JPEG2000 standard supports many unique features that were not possessed by previous image compression standards. Some of most relevant attributes to the materials of this thesis are presented in this section.

Error Resilience

Error resilience becomes crucial as wireless communication becomes more prominent and wireless channels remain highly error prone. An arithmetic coder is used in JPEG2000 standard, which is a variable length coder, to compress the quantized wavelet coefficients. Although each code block is independently encoded and errors

constrained to that code block, variable length encoding causes severe distortion if the error unsynchronized the bit stream.

Error resilience in JPEG2000 is achieved through the ERTERM mode, the SEGMARK mode, or a combination of the two. Normally, the encoder may terminate code-word segments in any manner which complies with the standard. However, when the ERTERM is used a predictable termination policy must be followed. This helps the decoder to exploit the properties of the predictable termination policy for detecting errors occurred in bit-stream. Once a corruption detected in a code-word segment, the corrupted and all subsequent segments are discarded.

SEGMARK mode on the other hand, adds synchronization markers to the bit-stream. A string of four binary symbols must be encoded at the end of each bit-plane. The SEGMARK symbols are used to detect the presence of errors, since a single error in a bit-plane is likely to corrupt at least one of the four binary symbols. The decoder discards the corrupted coding passes (Figure 11). In the simple case, the truncated bit-stream is decoded, which results in a lower quality image, and yet the loss in quality is less than the visual artifacts produced by decoding a corrupted bit-stream.

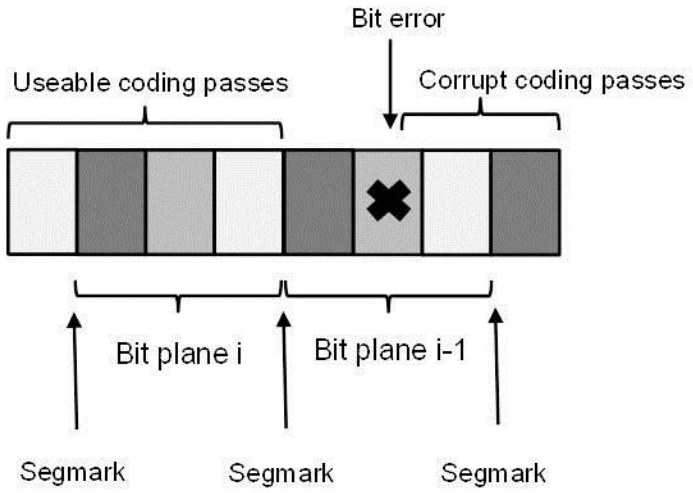

Figure 11. SEGMARK mode [15]

Scalability

One of the most interesting features of JPEG2000 standard is the supporting of scalability. The philosophy lies behind this feature is to compress the image once and decompress it in many ways to achieve more than one quality/resolution. On the decoding stage, truncation of the bit-stream at specific points results in obtaining lower qualities or resolutions of the original image.

The importance of this feature is that there is no need to know the target bit rate or reconstruction resolution at the time of compression. Additionally, another advantage of the scalability, which is more of our interest in this thesis, is the ability to increase the resistance toward transmission errors by providing different layers with different importance. This property of JPEG2000 is very important, since it prevents from the buildup of compression noise through repeated decompression cycles.

2.2. Related Works

As stated previously, our goal is to take advantage of OFDM-based cognitive radio network for efficient use of frequency resources with the proposed subcarrier and power allocation to transmit the multimedia bit-streams. A considerable amount of literature has been published on subcarrier and power allocation for transmission of data over OFDM-based cognitive radio [18]–[20]. These studies mainly concentrated on the maximization of the system throughput under resource constraints with the assumption that all information bits in the transmitted bit-stream are equally important. Applying the traditional schemes to the transmission of scalable multimedia bit-streams results in poor resource utilization [21]. Therefore, several attempts have been made to address this issue [22]–[25]. In [23], the authors optimized video streaming to exploit more channel resources for secondary user by developing a flexible sensing-transmission scheme. In [24], a cross-layer quality-aware resource allocation algorithm to optimize OFDM access-based (OFDMA-based) cognitive radio network performance was proposed, by considering the imperfect channel state information between the secondary user and primary user. It also considered quality-aware resource allocation using the H.264/AVC standard. The study in [25] proposed a bit-error-rate-driven (BER-driven) resource allocation for scalable bit-streams over OFDMA systems, which can be applied to the cognitive radio networks with some changes in the considered constraints.

In [26], the secondary users were numbered and two different channels were used to transmit the scalable video stream. In this scenario, secondary users with odd numbers transmited their base layer in the first channel and their enhancement layers in second channel. While, the secondary users with even numbers did the reverse, which was sending base layer in second channel and enhancement layers in first one. Therefore, the employed channel selection scheme balanced the base layers and enhancement layers over the channels, thus balanced the resource allocation. Scalable video coding and co-operative transmission features were both utilized in [27]. When the direct channel between the node and the base station did

not have a good condition, secondary user used other nodes as a link to the base station. To protect the rights of subscribed secondary users, only enhancement layers were transmitted through other nodes, so that other nodes could not reconstruct the video stream and the base layer transmitted directly to the base station.

Authors in [28], used a hybrid system, that is transmitting data with both overlay and underlay schema to transmit the scalable video stream. Only enhancement layers with lower importance in video quality were sent with underlay method, base layer and other enhancement layers were sent with overlay method. As suggested in [29], joint design of distributed video coding (DVC) and cognitive radio provides a good solution to improve both resource utilization efficiency and QoS of video transmission. DVC uses the advantage of simple encoder, which makes it a suitable choice for wireless video applications. The need for the large network resource can be fulfilled by cognitive radio. Using the cognitive radio, the video stream is transmitted to the nearest base station first, where the stream decoded and reencoded, this time with high complex encoder. The video stream then is sent to the receiver end.

Dynamic nature of cognitive radio requires efficient dynamic channel selection. The work in [30] provided an efficient model of wireless environment and estimated the delay of video packet transmission when selecting a specific frequency channel. Then by applying the priority virtual queuing for users, adapted their channel selection and maximized video quality.

There are some other works in this area with a focus on other cognitive radio aspects rather than efficient resource allocation and output quality maximization. As an example of such studies, the work in [31] illustrated the impact of spectrum sensing frequency and the packet loading scheme on multimedia transmission over cognitive radio. The cognitive transceivers can only do one task at a time. Increase in frequency sensing may cause packets to miss the transmission deadline and

decrease the video quality. Using channel availability time and remaining packets as QoS factors, they derived a model between spectrum sensing and mentioned factors.

As suggested in [32], removing the redundancies via data compression leads to bandwidth saving, but it increases the sensitivity of the data to transmission errors. JPEG2000 standard has a quality progression feature, which can improve the received image quality progressively as more data from different quality layers are received [17]. In order to improve the transmission performance, the important parts of the bit-stream (lower layers) should transmit under more protection than less the important parts. This is known as unequal error protection [25], [33], [6], [34], [35].

Chapter 3.

Sub-channel Allocation for JPEG2000 Image Transmission over OFDM-Based Cognitive Radio Networks

Transmission and source allocation over frequency selective channels with OFDM-based cognitive radio has been widely investigated in the literature, as discussed in 2.2. Most of these works concentrated on the maximization of the throughput of the system under resource constraints with the assumption that all information bits in the transmitted bit-stream are equally important, which results in poor resource utilization for transmission of scalable multimedia bit-streams. In this chapter a channel allocation method based on JPEG2000 and OFDM features is proposed, which improves the quality of the secondary user's received image by providing dynamic access to the available spectrum, without violating the interference requirements of the primary user.

3.1. System Model

The overall system block diagram is presented in Figure 12, where the first block is to transform the format of an input image into the JPEG2000 format. Then the Structural Information Retrieval unit extracts the header information from data segment of the code-stream. This information is assumed to be transmitted and received error-free, and provides information about the number of layers, code-blocks and coding passes within each code-block.

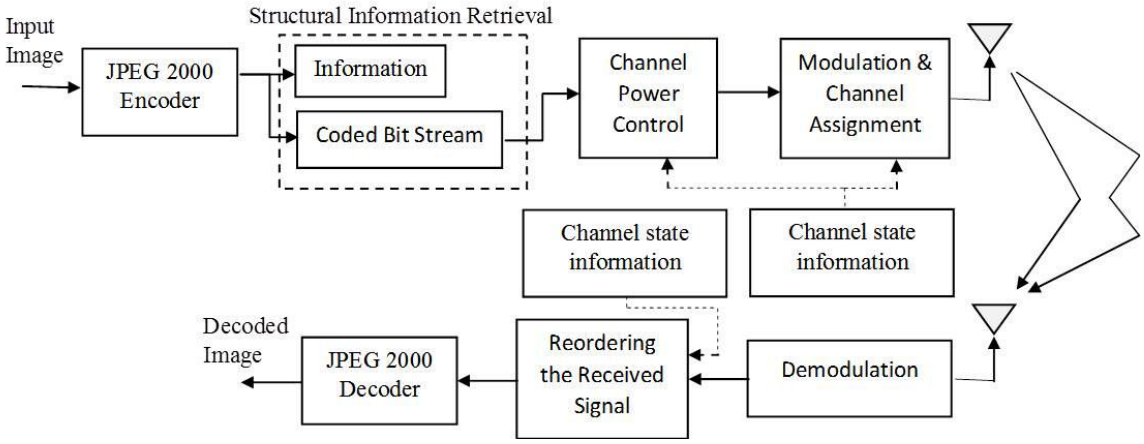

Figure 12. General block diagram

The next block performs channel and power allocation based on the available channels to the secondary user. The cognitive base station detects the channel gain of each subcarrier and has a perfect knowledge of the CSI between the primary user and secondary user. The CSI, which is assumed to remain unchanged during the transmission of each block, is provided to the power adjustment and channel allocation units. Once the instantaneous CSI is received, the Power Adjustment unit uses the instantaneous CSI to calculate the actual power of each bit in the n_{th}transmission block and produce the diagonal matrix $\mathbf{E}n$.

When all channels are available to the secondary user, power is equally allocated to each channel. In the case that the primary user occupies some of the sub-carriers, the Power Adjustment unit assigns power to the remaining channels such that the interference on the primary user is kept below a given threshold. The power is assigned to the channels and the bits are assigned to the channels based on their importance. In other words, the bits that highly affect the image quality are transferred trough channels with higher power and channel gain, while as power and channel gain decrease less important bits are transferred.

A serial to parallel buffer is considered in the OFDM transmitter for dividing the bit-stream, which is obtained from the JPEG2000 encoder, into $N_B$parallel blocks

$x_n = [x_1, x_2, \dots, x_N]^T$, where n=1,2,...,N_B. To form OFDM blocks, data in the channels that are occupied by primary user are considered to be zero and JPEG2000 bit-stream is reordered based on the channel allocation algorithm. Vector S_n is obtained by multiplying the power profile and data corresponding to each block, $S_n = \sqrt{\boldsymbol{E_n}} x_n$, in which E_n is a diagonal matrix of order *N*, where N is the number of subcarriers in the OFDM transmitter. The diagonal elements of the matrix E_n are the actual power of the bits in vector x_n [33].

For modulating the N subcarriers by the bit-stream, Inverse Fast Fourier Transform (IFFT) is applied to the elements of S_n to form $y_n = Q^H S_n$, where $(.)^H$ denotes complex conjugate transpose operation. The orthogonality between the subcarriers is ensured by keeping apart the adjacent subcarriers in y_n exactly by one cycle. The lower rate parallel subcarriers provide higher symbol duration, which lessens the relative amount of dispersion in time caused by the multipath delay spread. This, in addition to introducing a guard time in every OFDM symbol, eliminates ISI [36]. A cyclic prefix is added to the beginning of each OFDM symbol (y_n), to form the transmitting sequence, z_n , with a size of $N + m$. The transmission block format of OFDM symbols is shown in Figure 13, where the cyclic prefix consists of the last m symbols of every OFDM block ($m < N$).

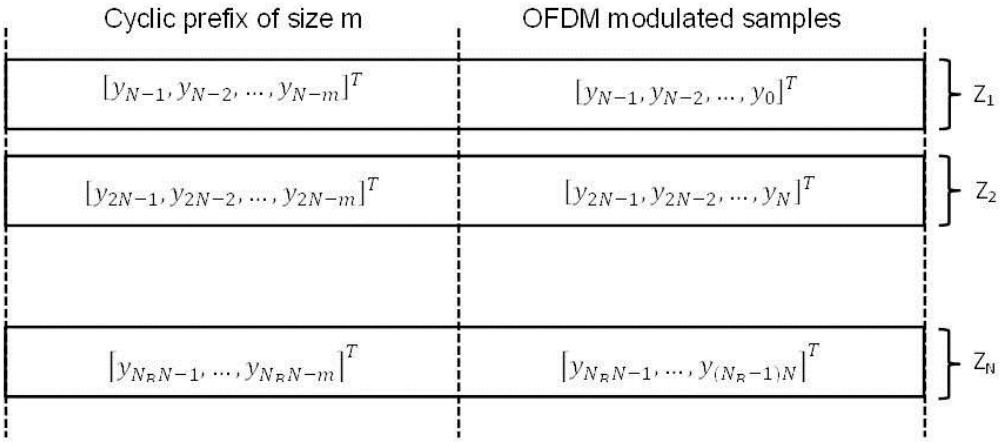

Figure 13. Transmission block format of OFDM symbols

A frequency selective fading channel model is assumed in this work. Matrix of Channel Impulse Response (CIR) for the n_{th} transmission block is constructed from independent zero-mean complex Gaussian random variables that remain constant over a single data block and vary independently for every block, i.e., $h_n = [h_0, h_1, h_2, \ldots., h_{m-1}]^T$ where m is the channel memory length and n *=1,2,…,*N_B. The received signal at the destination terminal is given by:

$$r_n = H_n Q^H \sqrt{E_n} x_n + v_n \tag{3.1}$$

In Eq. (3.1) r_n is the n_{th} received block of data, H_n is an $N \times N$ circulant matrix for the n_{th} transmission block with entries $[H_n]_{ik} = [h_n]_{(i-k) \bmod N}$ and $[h_n]_i = 0$ for $i > m-1$. $\mathbf{v}_n$ is an $N \times 1$ Additive White Gaussian Noise (AWGN) vector with mean of zero and variance of 1/2 per dimension. The channel structure in (3.1) is formed as a circulant matrix, which accounts for the addition of the cyclic prefixes to the OFDM symbols ($\boldsymbol{y}_n$).

The OFDM receiver transforms the received samples to the frequency domain by applying the Fast Fourier Transform (FFT), i.e, multiplying by the Q matrix.

$$Qr_n = \Lambda_n \sqrt{E_n} x_n + Qv_n \tag{3.2}$$

where $\Lambda_n = QH_nQ^H$ is a diagonal matrix of size $N \times N$ for the n_{th} transmission block, in which the diagonal elements are [37]:

$$\left[\Lambda_n\right]_{ii} = \sqrt{N} q_i^H \left(h_n \quad \overbrace{0 \quad \cdots \quad 0}^{N-m} \right)^T, \qquad \mathrm{i} = 1, 2, \cdots, \mathrm{N} \tag{3.3}$$

where q_i is the i_{th} column of the matrix Q. Due to the different realizations of the CIRs for each block of data, the diagonal elements of Λ change for every block n of the received signal, and they can be considered as the gains of an equivalent slow flat fading channel. Moreover, these elements are in fact the eigenvalues of the channel matrix $\mathbf{H}$. Overall, note that OFDM converts the underlying frequency selective channels into parallel flat fading channels [37].

One of the advantages of our proposed system is that the recovered data does not need a dedicated source decoder and can be decoded by any standard JPEG2000 decoder. More details on the system blocks and the receiver side will discuss in the following sections.

3.2. Matrix Representation of OFDM

In this work, the simulation is built based on a matrix representation of the OFDM system. Here the matrix representation of OFDM is explained. Considering the output equal to $y[n] = \tilde{x}[n] * h[n] + n[n]$, matrix representation of the output sequence can be written as

$$\begin{bmatrix} y_{N-1} \\ y_{N-2} \\ \vdots \\ y_0 \end{bmatrix} = \begin{bmatrix} h_0 & h_1 & \cdots & h_\mu & 0 & \cdots & 0 \\ 0 & h_0 & h_1 & \cdots & h_\mu & \cdots & 0 \\ \vdots & \ddots & \ddots & \ddots & \ddots & \ddots & \vdots \\ 0 & \cdots & 0 & h_0 & \cdots & h_{\mu-1} & h_\mu \end{bmatrix} \begin{bmatrix} x_{N-1} \\ \vdots \\ x_0 \\ x_{-1} \\ \vdots \\ x_{-\mu} \end{bmatrix} + \begin{bmatrix} v_{N-1} \\ v_{N-2} \\ \vdots \\ v_0 \end{bmatrix} \tag{3.4}$$

which can be written in more compact form of

$$y = Hx + v \tag{3.5}$$

The received symbols y_{-1}, $\cdots$, $y_{-\mu}$ can be discarded, since they are affected by ISI in the prior data block, and there is no need for these symbols for input recovery. The last μ symbols of $x[n]$ correspond to the cyclic prefix: $x_{-1} = x_{N-1}$, $x_{-2} = x_{N-2}$, $x_{-\mu} = x_{N-\mu}$. Therefore, it can be inferred that the previous matrix representation is equivalent to the following representation

$$\begin{bmatrix} y_{N-1} \\ y_{N-2} \\ \vdots \\ y_0 \end{bmatrix} = \begin{bmatrix} h_0 & h_1 & \cdots & h_\mu & 0 & \cdots & 0 \\ 0 & h_0 & h_1 & \cdots & h_\mu & \cdots & 0 \\ \vdots & \ddots & \ddots & \ddots & \ddots & \ddots & \vdots \\ 0 & \cdots & 0 & h_0 & \cdots & h_{\mu-1} & h_\mu \\ \vdots & \ddots & \ddots & \ddots & \ddots & \ddots & \vdots \\ h_2 & h_3 & \cdots & h_{\mu-2} & \cdots & h_0 & h_1 \\ h_1 & h_2 & \cdots & h_{\mu-1} & \cdots & 0 & h_0 \end{bmatrix} \begin{bmatrix} x_{N-1} \\ x_{N-2} \\ \vdots \\ x_0 \end{bmatrix} + \begin{bmatrix} v_{N-1} \\ v_{N-2} \\ \vdots \\ v_0 \end{bmatrix} \tag{3.6}$$

With the compact form of

$$y = \tilde{H}x + v \tag{3.7}$$

The channel is modeled as a circulant convolution matrix $\tilde{H}$ over the N samples of interest based on this representation. The matrix $\tilde{H}$ is $N \times N$, so it has an eigenvalue decomposition.

$$\tilde{H} = M \Lambda M^H \tag{3.8}$$

where Λ is a diagonal matrix of eigenvalues of $\tilde{H}$ and M^H is a unitary matrix whose rows comprise the eigenvectors of $\tilde{H}$. It is straightforward to show that the DFT operation on $x[n]$ can be represented by the matrix multiplication

$$X = Qx \tag{3.9}$$

and Q is a $N \times N$ matrix given by

$$Q = \frac{1}{\sqrt{N}} \begin{bmatrix} 1 & 1 & 1 & \cdots & 1 \\ 1 & W_N & W_N^2 & \cdots & W_N^{N-1} \\ \vdots & \ddots & \ddots & \ddots & \vdots \\ 1 & W_N^{N-1} & W_N^{2(N-1)} & \cdots & W_N^{(N-1)^2} \end{bmatrix} \tag{3.10}$$

For $W_N = e^{-\frac{j2\pi}{N}}$ the following equation is true.

$$Q^{-1} = Q^H \tag{3.11}$$

The IDFT can be similarly represented as

$$x = Q^{-1}X = Q^H X \tag{3.12}$$

It can also be shown that the rows of the DFT matrix Q are eigenvectors of $\tilde{H}$, which implies that $Q = M^H$ and $Q^H = M$. Thus the following equations are driven.

$$
\begin{aligned}
Y &= Qy \\
&= Q\left[\tilde{H}x + v\right] \\
&= Q\left[\tilde{H}Q^{H}X + v\right] \\
&= Q\left[M\Lambda M^{H}Q^{H}X + v\right] \\
&= QM\Lambda M^{H}Q^{H}X + Qv \\
&= M^{H}M\Lambda M^{H}MX + Qv \\
&= \Lambda X + Qv
\end{aligned}
\tag{3.13}
$$

Thus, this matrix analysis also shows that by adding a cyclic prefix and using the IDFT/DFT, OFDM decomposes an ISI channel into *N* orthogonal sub-channels and knowledge of the channel matrix *H* is not needed for this decomposition.

3.3. Power Calculation

As shown in [24], [38], due to the non-orthogonality of primary and secondary transmitted signals, an interference between the primary user and secondary user sub-channels exists that is caused by the side lobes of the OFDM signal. This interference is shown in Figure 14.

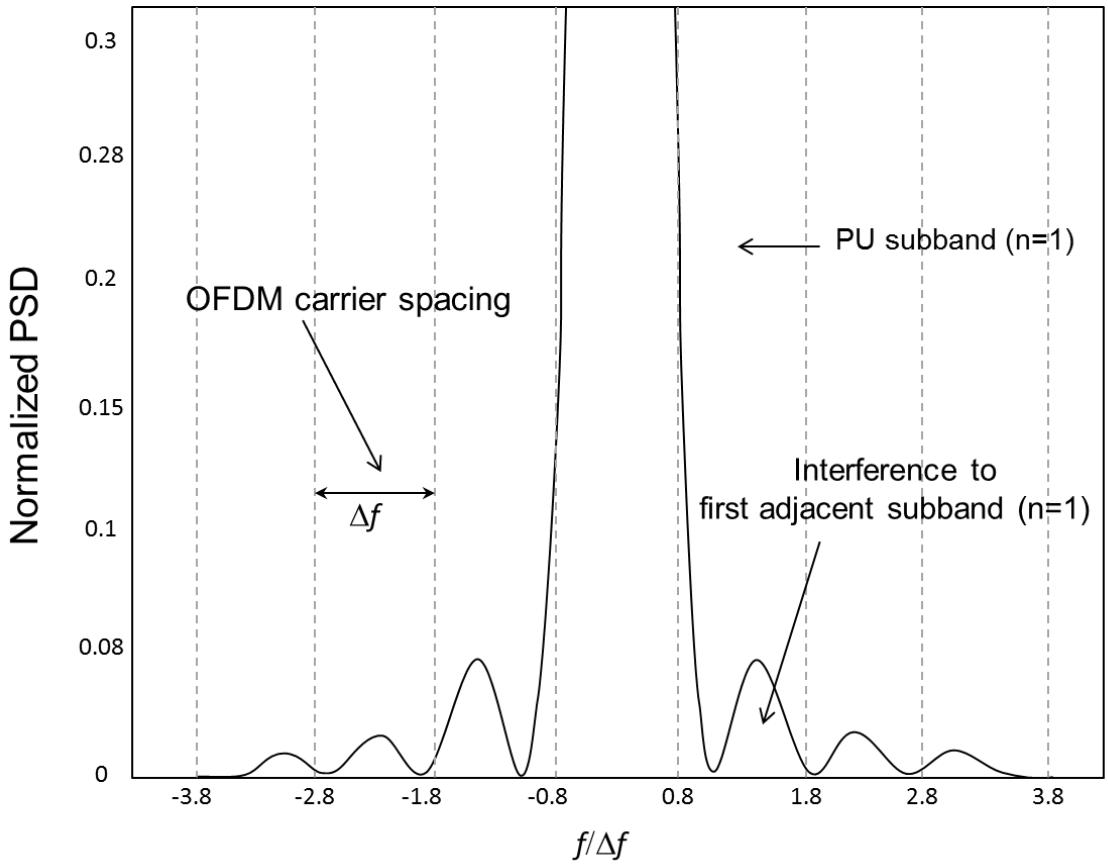

Figure 14. PSD of a single OFDM modulated carrier in IEEE802.11a

To calculate this interference, which is called mutual interference, the Power Spectral Density (PSD) of the transmitted signal is required. The PSD of a transmitted signal in each subcarrier is found by Eq.(3.14), in which P_n is the transmitted power allocated to the n_{th} sub-channel, and T_s is the symbol duration.

$$\Phi_n(f) = p_n{}^2 T_s \left(\frac{\sin(\pi f T_s)}{\pi f T_s} \right)^2 \tag{3.14}$$

Substituting Eq.(3.14) into Eq.(3.15), the interference on primary user's channel, caused by the subcarrier, can be obtained. In Eq.(3.15), d_n is the spectral distance between the central frequency of subcarrier n and the primary user, B_n is

the bandwidth occupied by the primary user, and h^{SP} denotes the channel gain between the secondary user transmitter and the primary user receiver.

$$I_n = \left|h^{SP}\right|^2 \int_{d_n - \frac{B_n}{2}}^{d_n + \frac{B_n}{2}} \Phi_n(f)df \tag{3.15}$$

The total interference that the primary user experience is calculated by Eq.(3.16). This interference needs to be limited to an allowable level, I_{th}, set by the primary user.

$$I_{Total} = \sum_{n=1}^{N} I_n \tag{3.16}$$

3.4. Channel Allocation

In this section, a sub-channel allocation algorithm is proposed based on the allocated power to each sub channel and the channel status, *cf.* Table 2. The decision making parameter used in this algorithm is γ, defined as:

$$\gamma = P_k h_k^{SS} \tag{3.17}$$

In Eq.(3.17), h_k^{SS} shows the channel gain of the secondary users K_{th} sub-channel between the transmitter and receiver. Higher γ values mean more secure and reliable transmission of data, which make the corresponding channel more appropriate for sending the important JPEG2000 bits.

In the sub-channel allocation algorithm, because of the quality layered structure of JPEG2000, the coded bit stream can be divided into two groups. One group contains coded bits with more significant contribution in the quality of the received image G_1 while

the other contains the remaining bits G_2. A threshold, , equal to 1/2max{γ} is chosen. For sub-channels with $\gamma > C_{th}$, data from the most significant bit group G_1 is sent and for the channels with $\gamma < C_{th}$, data from the less significant group G_2 is sent.

As each OFDM symbol is sent, the number of transmitted symbols must be counted to keep track of transmitted and remaining bits of each group. If $\gamma > C_{th}$, after sending all of the data from the significant group, data from the less significant group is sent accordingly. In the case where $\gamma < C_{th}$, the opposite events occur. This way we can avoid any decrease in the system throughput, which is an important factor in cognitive radio.

Table 2. Channel allocation algorithm

Algorithm 1
1. Splitting the coded bit stream into two groups: G_1 and G_2 with the size of N_1 and N_2;
2. Selecting the threshold parameter, C_{th};
3. Calculating γ for each sub-channel;
4. Reordering the data to generate OFDM symbol by comparing the γ value with C_{th};
5. Setting the counter n_1=0 for G_1, and n_2=0 for G_2;
6. If $C_{th} < \gamma$ and $n_1 \geq N_1$, send data from G_2 in that sub-channel and set $n_2=n_2+1$;
7. If $C_{th} < \gamma$ send $n_1 < N_1$, data from G_1 in that sub-channel and set $n_1=n_1+1$;
8. If $C_{th} > \gamma$ and $n_2 \geq N_2$, send data from G_1 in that sub-channel and set $n_1=n_1+1$;
9. If $C_{th} > \gamma$ and $n_2 < N_2$, send data from G_2 in that sub-channel and set $n_2=n_2+1$;

One of the assumptions in the proposed algorithm is that the channels state information and their availability are known to the SU transmitter and receiver a priori; and the data will be transmitted with the highest possible power, unless the PU appears.

Implementing these assumptions will lead to the receiver getting significant data from channels with greater γ values. Since the channel condition and Signal to Noise Ratio (SNR) is also available for the receiver, it can predict the interference generated by each sub-channel and hence the order of received bits, considering the fact that the number of bits in each group is known to the receiver.

3.5. Simulation Results

To assess the proposed method, grayscale images of size 512×512 and 8 bit/pixel are used for transmission and the Kakadu software is utilized as the JPEG2000 image coder. The images are processed with one level of decomposition and are divided into 64×64 CBs and 128×128 precincts. For the baseline scenario, 16 sub-carriers, one PU, and one SU is considered. Table 3 shows the selected values for the model parameters based on the IEEE 802.11a standard [39].

Table 3. Model parameters

Parameter	Value
Symbol duration, T_s (μs)	4.0
Subcarrier's occupied bandwidth, Δf (MHz)	0.3125
Primary user band width, B_{PU}	5.0

A frequency selective fading channel is considered. Slow fading channels are assumed to be used here.

The average peak signal to noise ratio (PSNR) at the SU receiver for various SNRs is used to indicate the decoded image quality. The relationship between PSNR and mean square error, MSE between original and decoded image, is presented in Eq.(3.18), in which 255 is the maximum possible pixel value of the 8-bit test images.

$$PSNR = 10\log_{10}\left(\frac{255^2}{MSE}\right) \tag{3.18}$$

The average PSNR at the receiver for the secondary user at various SNRs for two channels with different memories is plotted in Figure 15. Comparison is made between the system using the proposed algorithm and a system which sends the coded image without any reordering based on channel condition and interference to primary user. The simulation is done for two different channel memories. In both cases, for very low SNRs (< 5), the proposed technique does not make a significant improvement to the average PSNR; however, the average PSNR starts to increase gradually as the SNR goes beyond 5. The increasing trend of the improvement in the PSNR continues up to SNR values close to 15. This can be observed more clearly in Figure 19, where the difference in the PSNR with and without the application of the present algorithm is plotted at various SNRs. There is a peak of the plotted curve in Fig. 5 showing that maximum improvement is achieved at SNRs in the range of 15 to 20 dB. Since SNR is a representative of power, this shows a potential to optimize the data transmit with respect to the assigned power. It can also be inferred from Figure 15 and Figure 19 that the improvement is more pronounced when the number of channel taps is smaller. A slight degradation in PSNR is expected by increasing the number of channel taps, since the amount of available power to the data bits is reduced because of extra power required for the cyclic prefix.

Plotted in Figure 16 is the BER for the two considered cases (i.e., with and without application of the proposed algorithm). As expected, there is no difference in the average BER in these two cases, what is different, however, is that the proposed system provides higher protection for bits with higher significant in the quality of the received image, by transmitting them over stronger sub-channels.

Similar results are obtained from analysis of Peppers image, shown in Figure 17 and Figure 18.

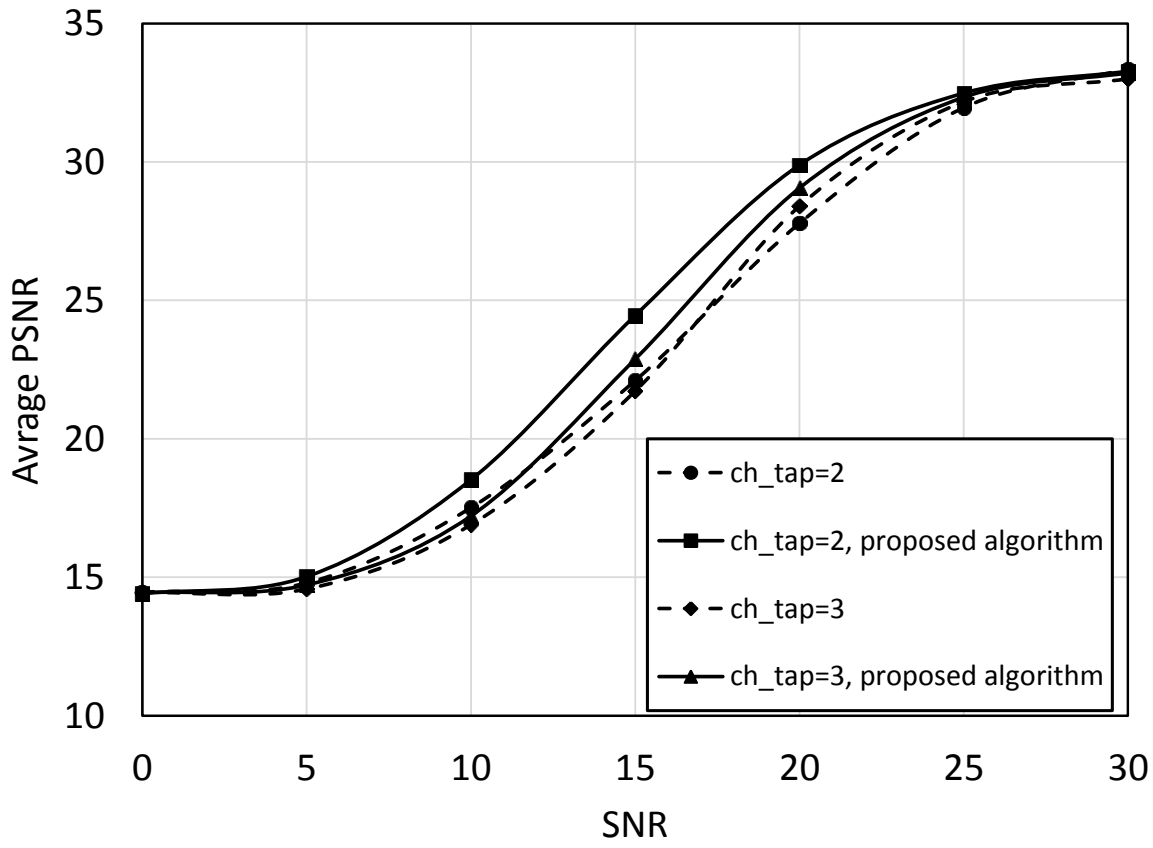

Figure 15. Average PSNR value versus SNR value for two different channel memories of the received "Lenna"

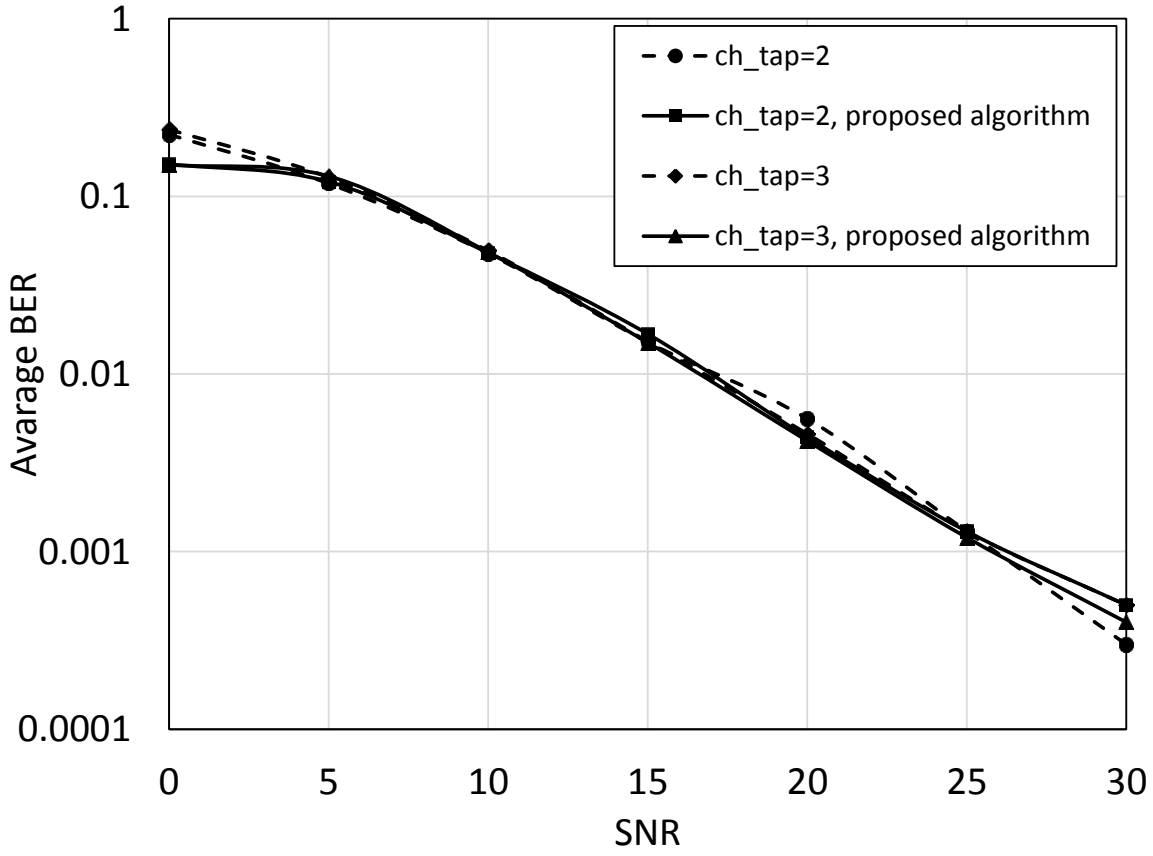

Figure 16. Average BER value versus SNR value for two different channel memories of the received "Lenna"

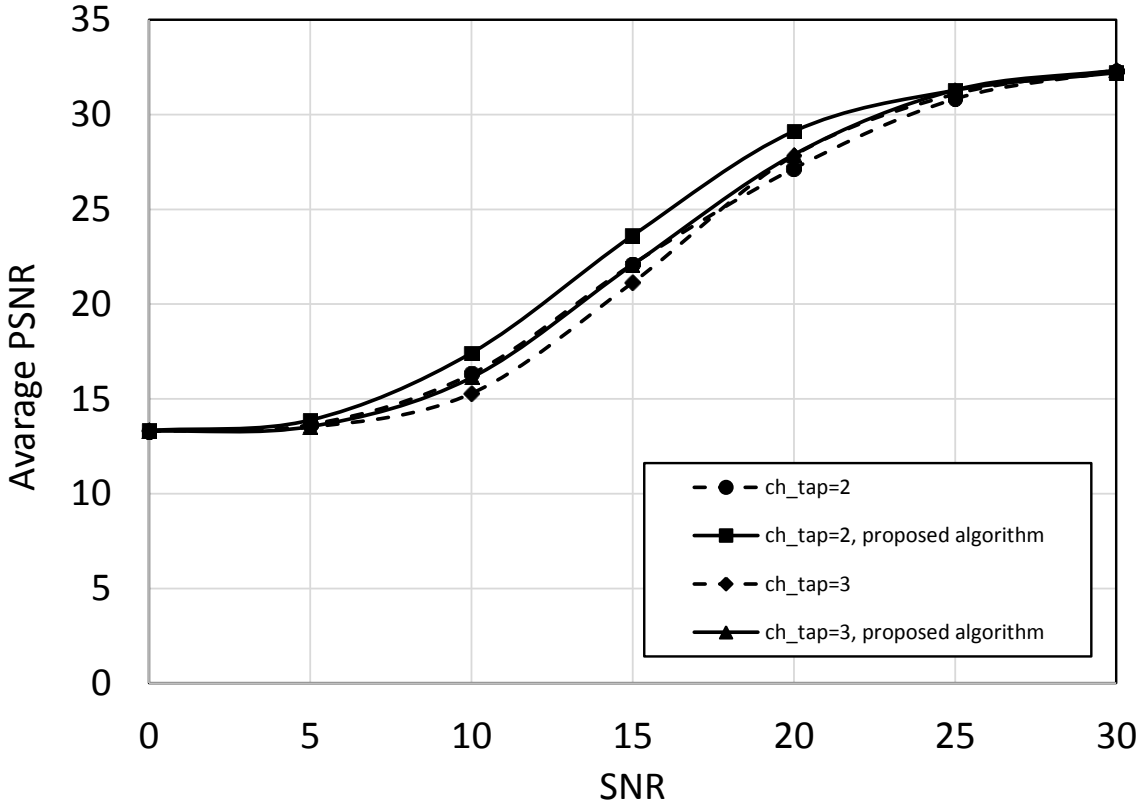

Figure 17. Average PSNR value versus SNR value for two different channel memories of the received "Peppers"

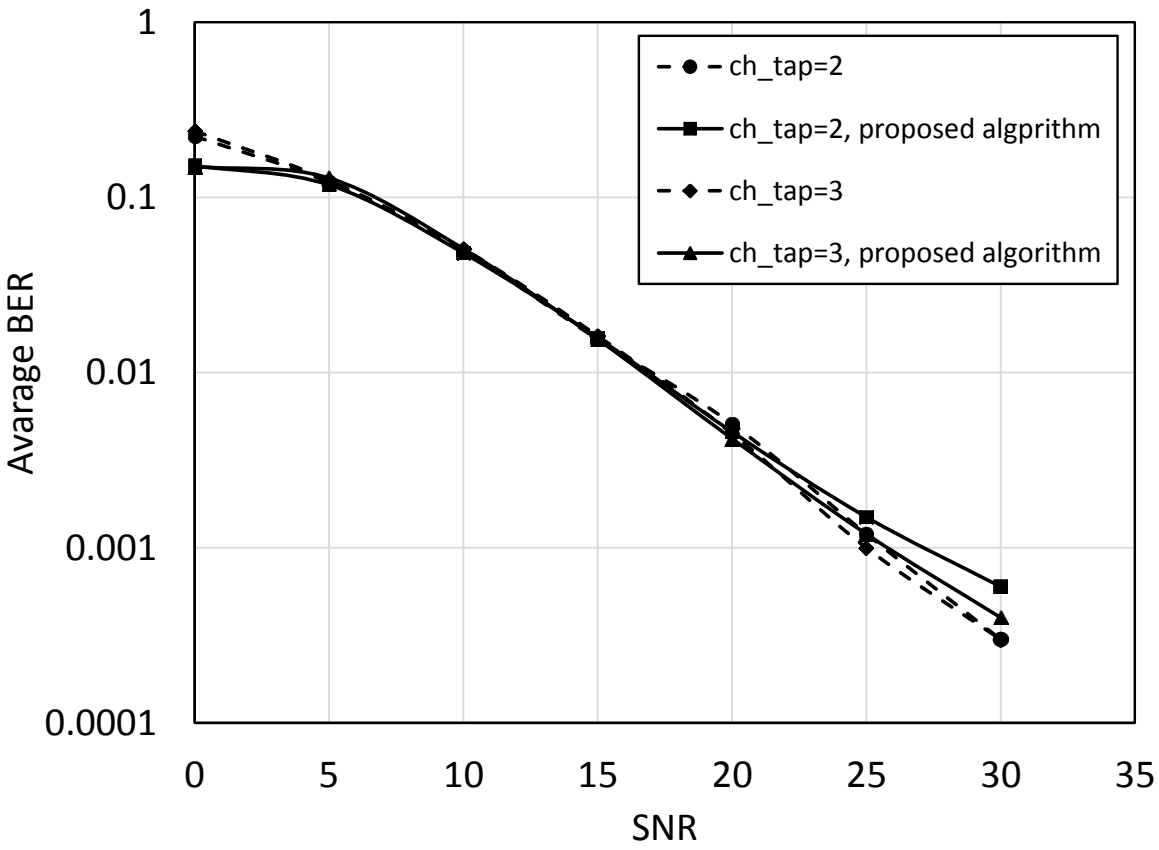

Figure 18. Average BER value versus SNR value for two different channel memories of the received "Peppers"

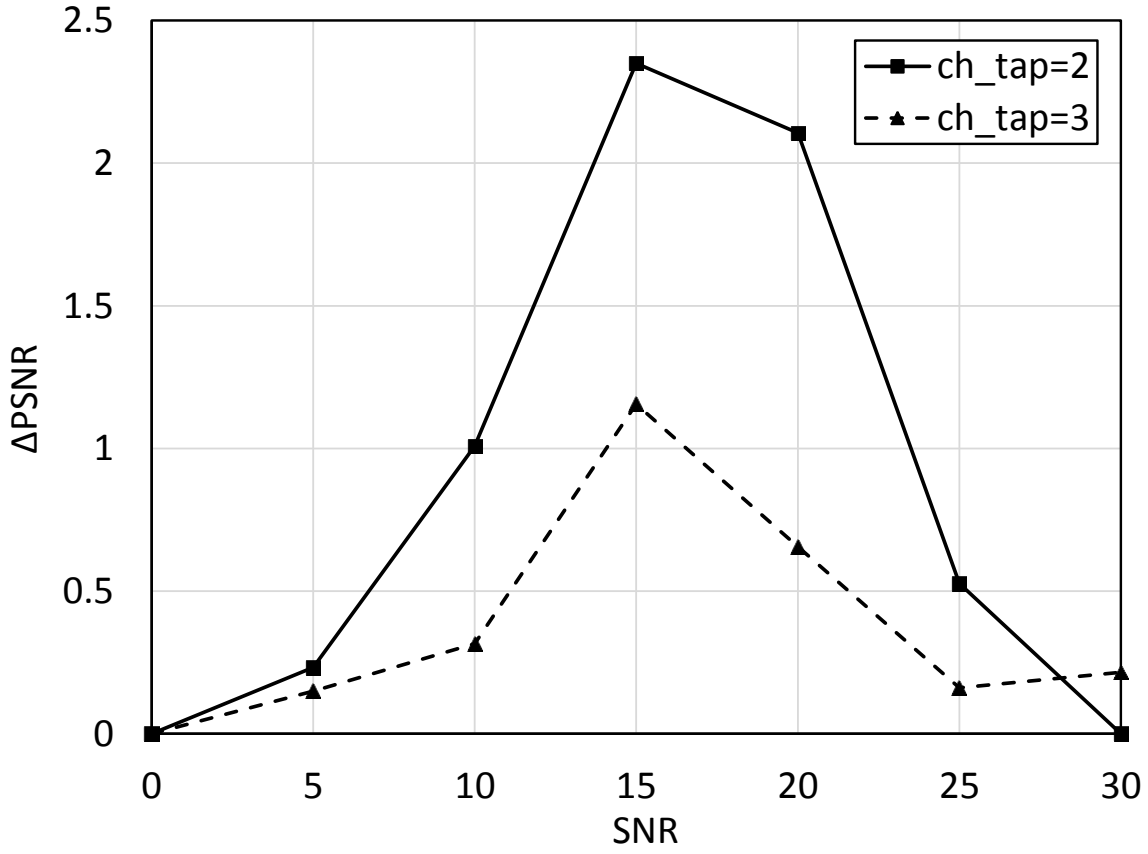

Figure 19. The improvements in the PSNR value at various SNR for two different channel taps of the received Lenna.

For better visual comparison, received images of Lenna and Peppers without applying the algorithm are shown in Figure 20(a) and Figure 21(a) and the same image by applying the algorithm are shown in Figure 20(b) and Figure 21(b).

(a)

(b)

Figure 20. Visual comparison of "Lenna", transmitted at SNR=15,where (a) is the reconstructed image in 2 tap channel and (b) is the reconstructed image in 2 tap channel applying the proposed algorithm.

(a)

(b)

Figure 21. Visual comparison of "Peppers", transmitted at SNR=15,where (a) is the reconstructed image in 2 tap channel and (b) is the reconstructed image in 2 tap channel applying the proposed algorithm.

3.6. Summary

In this chapter, a novel algorithm was proposed to improve the resource allocation for transmission of JPEG2000 codec over OFDM based cognitive radio. In this algorithm, OFDM symbols were created by reordering the JPEG2000 bit-streams based on the importance of data and channel status. The developed algorithm was observed to improve the secondary user's PSNR value without violating the primary user's interference limit. To assess the proposed approach, the algorithm was applied to image transmission according to IEEE 802.11a conditions. It was observed that this new technique can enhance the average PSNR significantly for multipath channels with two and three taps. However, the obtained improvements in the average PSNR for the two-tap channels were more sizable. Additionally, a peak of the PSNR improvement-SNR curve was found that shows there is an optimum SNR value where the PSNR improvement is a maximum. This information can be helpful in designing high efficiency cognitive radio systems, in terms of power consumption.

This chapter is the result of works published in [6].

Chapter 4.

Power and Sub-channel Optimization of JPEG2000 Image Transmission over OFDM-Based Cognitive Radio Networks

One of the main constraints in wireless communication is the limitation in power. Therefore, power allocation is one of the important factors needs to be considered along with other resource allocation. Numerous studies have attempted to propose an efficient power allocation method for wireless communication over cognitive networks, and as it is shown in [5], equal power allocation gives the least performance. In this chapter, we improve the received image quality in a cognitive radio system by taking advantage of the scalable bit-stream and application of UPA in two stages. The first stage optimizes the power allocated to the JPEG2000 bit-stream at the coding pass level to minimize the total received distortion. The second stage employs subcarrier allocation, adaptive modulation, and power adjustment to meet the interference requirements, based on channel conditions, and at the same time keeps the same throughput for the system. This strategy is expected to enhance the image quality, since important parts of the image will be transmitted more reliably.

4.1. System Model

The overall system block diagram of the proposed scheme is shown in Figure 22, where the functionality of the first block, JPEG2000 encoder, and structural information retrieval unit are well explained in section 3.1. The next block performs the

UPA optimization algorithm on the coded bit-stream of the JPEG2000 image, where an optimal amount of power is allocated to each bit in order to minimize the total distortion

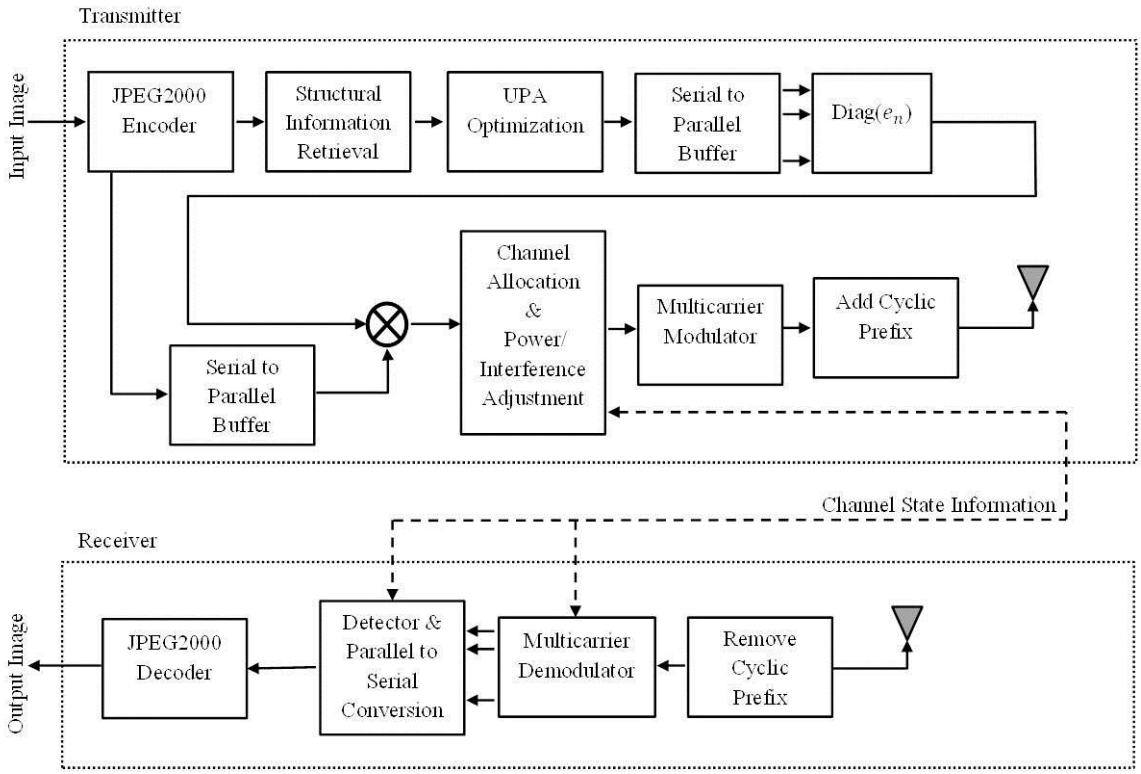

Figure 22. General block diagram

of the received image. The output of this block is a vector that contains the optimized power to be allocated to each bit in the code stream. A serial to parallel buffer divides the obtained vector into several blocks of size N, where N is the number of subcarriers in the OFDM transmitter. The CSI, which is assumed to remain unchanged during the transmission of each block, is provided to the power adjustment and cannel allocation units. The channel allocation unit will choose the optimum subcarrier for sending the important layers and the power adjustment unit will use the CSI to calculate the mutual interference and perform the required adjustment. Transmission of bit-stream occurs via an OFDM-based transmitter, and an adaptive modulation is applied to maintain the system rate if the number of available sub-channels to the secondary user decreased. Each subcarrier has a bandwidth of $B_n = B_T / N$, which is assumed to be smaller than the

coherence bandwidth in the frequency selective wireless channel so that each subcarrier undergoes flat fading. The cognitive base station detects the channel gain of each subcarrier and has a perfect knowledge of CSI between the primary user and secondary user.

Since CSI is known in the transmitter and receiver sides, the received modulated symbols from each layer at the receiver side can be demodulated for each assigned subcarrier before forming a layer of bit-stream. The received layers are then merged into a single scalable bit-stream which will be sent to the JPEG2000 decoder.

One benefit of using JPEG2000 standard for coding image is its error resilience feature that improves the performance of transmitting a compressed image over error prone channels by stopping error from propagation beyond the code-block with corrupted bit-stream. This process is performed by including resynchronization markers. Additionally, code-blocks are encoded independently. As a result, the decoder is able to restart decoding from the next code-block if any error occurs, and the markers continuously synchronize the encoder and decoder [40]. Thanks to this feature of JPEG2000 standard, it is assumed in this work that the decoder prevents errors from propagating to the entire bit-stream.

4.2. Problem Formulation

Our objective for resource allocation is to maximize the quality of the received image by minimizing the distortion of the decoded JPEG2000 bit-stream under interference and power constraints. This problem can be formulated as follows:

$$\text{Minimize } E\{D_{Total}\}$$

$$\begin{aligned} \text{Subject to} \quad & P_{m,n} \geq 0 \ \ \forall n, m && (a) \\ & \sum_{m=1}^{N_B} \sum_{n=1}^{N} P_{m,n} \leq P_{Total} && (b) \\ & \sum_{n=1}^{N} r_{n,l} \geq R_l && (c) \\ & \sum_{n=1}^{N} I_n \leq I_{th} && (d) \end{aligned} \tag{3.19}$$

The parameters of Eq.(3.19) are listed in Table 4.

Table 4. List of Eq Parameters.

Parameter	Description
D_{Total}	Total distortion of the decoded image
$P_{m,n}$	Power assigned to channel n_{th} of m_{th} OFDM block
P_{Total}	Total available power for transmission of the image
N_B	Number of OFDM blocks
N	Number of OFDM subcarriers
$r_{n,l}$	Corresponding number of transmit bits per allocation period of subcarrier n for layer l
I_n	Interference on PU's channel, caused by the n_{th} subcarrier
I_{th}	Tolerable interference of primary user threshold

Since the CSI is available at the time of transmission, the above problem is solved in two stages. The first stage optimizes the power allocated to the JPEG2000 bit-stream at the coding pass level to minimize the total received distortion and the second stage employs subcarrier allocation and power adjustment to meet the interference requirements, and channels fading.

4.2.1. Objective Function

The expected value for the total distortion of the decoded image is formulated by[33]:

$$E\{D_{Total}\} = d_0 + \sum_{i=1}^{N_{CB}} \sum_{j=1}^{N_{CP,i}} p_{ij} D_{ij} \prod_{k}^{j-1} (1 - p_{ik}) \tag{3.20}$$

where, d_0 is the distortion caused by quantization during coding process, N_{CB} is the total number of code-blocks in the bit-stream, and $N_{CP,i}$ is the number of coding passes in the i_{th} code-block. p_{ij} is the probability of having at least one bit error in the j_{th} coding pass in the i_{th} code-block (i.e., CP_{ij}). Note that p is used to indicate the probability, while P represents the power throughout this thesis. D_{ij} is the distortion caused by any bit error in CP_{ij}. The parameters N_{CB} and $N_{CP,i}$ are extracted from the JPEG2000 encoder by the structural information retrieval block in Figure 22, and are provided to the UPA unit to compute the distortion.

In Eq.(3.20), d_0 is defined as the mean-square error (MSE) between the original image (distortion-free) and its decoded version, assuming zero fading and noise, and is thus due to only the quantization error caused by the encoder. The distortion corresponding to each coding pass (i.e., D_{ij}), is obtained by manually altering at least one bit in CP_{ij}, while the rest of the image bit-stream is kept error-free. D_{ij} is then determined by finding the MSE between the decoded and the original images. It should be noted that the distortion caused by an erroneous coding pass is the same, regardless of the number and positions of bit errors in that coding pass, as long as there is at least one bit error in that coding pass. In other words bits within the same coding pass have equal contribution to the quality of the received image. Therefore, in our algorithm, equal power is allocated to all bits within the same coding pass, which leads to identical error probability for all bits within a specific coding pass. Thus, p_{ij} can be found from Eq.(4.3).

$$p_{ij} = 1 - \left(1 - p_{eb}(i,j)\right)^{N_b(i,j)} \tag{3.21}$$

where, $p_{eb}(i, j)$ and $N_b(i, j)$ are the BER and the number of bits in CP_{ij}, respectively.

Due to our earlier assumption of AWGN channel for the optimization problem formulation, $p_{eb}(i, j)$ is the BER in the AWGN :

$$p_{eb}(i, j) = \mathcal{Q}\left(\sqrt{\frac{2P_{ij}}{N_0}}\right) \tag{3.22}$$

where, P_{ij} is the assigned power to each bit within $CP_{ij,}$ N_0 is the noise power, and Q(.) is the Q function. The application of necessary power adjustments, due to the presence of fading, is performed by the power adjustment unit shown in Figure 22, as discussed in [33]

4.2.2. Constraints

In the optimization problem formulated in Eq.(3.19), the first constraint, Eq.(4.1.a), is due to the fact that power is always positive. The second constraint, Eq.(4.1.b), applies a limit to the total available power, P_{Total}, for transmission of the image. Here, N_B is the number of transmitted OFDM blocks, and $P_{m,n}$ is the adjusted power assigned to the n_{th} subchannel of the m_{th} OFDM symbol.

The third constraint, Eq.(4.1.c) presents the rate constraint, where $r_{n,l}$ is the corresponding number of transmit bits per allocation period of subcarrier n for layer l, which can be calculated from Eq.(4.5) [25].

$$r_{n,l} = \log_2\left(1+\alpha_l h^{SS} P_{n,m,l}\right)\times\left(\frac{\tau}{T_s}\right) \tag{3.23}$$

h^{SS} in Eq.(3.23) shows the channel gain of the secondary user's n_{th} subchannel between the transmitter and receiver, which is assumed to remain constant during each

allocation period τ due to slow Rayleigh fading. α_l is also a coding loss factor related to the target BER of layer l by adapting quadrature amplitude modulation.

How to calculate the interference, which is the last constraint in this problem is explained in detail in section 3.3.

4.3. Unequal Power Allocation

The objective function in Eq.(3.19) is not a convex function. Therefore, to solve the UPA problem as suggested in [41], Simulated Annealing (SA) method is used to locate an acceptable approximation of the global minimum in a large search space. Due to the large number of coding passes and different number of bits in each coding pass, calculating the optimum value of power for every single coding pass in the bit-stream is computationally extensive. Hence, coding passes are divided into *L* different groups and the SA optimization algorithm is applied to find the optimum value of power for each group of coding passes. A smaller number of groups lessens system complexity while reduces algorithm accuracy; therefore, there is a tradeoff between the two. Testing the algorithm for transmission of Lenna (512×512, 0.25 bpp) with different number of groups (L) in various values of SNR, it was observed that the performance improves with the number of groups L; however, the improvement in performance was not significant as the number of groups exceeded 10. As a result the number of groups was proposed to be 10 in [41], and the same value is used here.

In Simulated Annealing (SA) algorithm, first an initial column vector of size L, $P_{initial}$, is considered as the power for different bits in each group. For each iteration of the algorithm, a new power distribution, P_{new}, is calculated using the following formula:

$$P_{new} = P_{current} + \left(\varepsilon - \frac{iter}{iter_{\max}} \right) \times \frac{P_{Total}}{L} z \tag{3.24}$$

In Eq.(3.24), *iter* is iteration number, *itermax* is the maximum number of iterations, L is the number of groups, and $z = [z_1, z_2, \ldots, z_L]^T$ is a uniformly distributed random vector between (−β,+β). It is found in [33] that the algorithm is not sensitive to the constant parameters ε and β. Therefore, in this paper ε and β are set to 1.5 and 0.1, respectively. The expected distortion resulting from the new values is then checked to see whether it is a potential minimum or not. The absolute minimum of distortion is finally found through an iterative procedure that determines the power for each group [33].

The summary of the implemented algorithm is shown in Table 5. Due to the nature of Eq.(3.24), the SA optimization algorithm needs to search for the solution in a large domain and finds the neighboring values from a wide random range; however, by progressing in iterations, the search space gets narrower. In order to avoid sticking to local minima, an uncertainty with a specific probability (which is set to be 0.05) is added to the line 14 of the algorithm. Moreover, in the SA optimization algorithm, the power is normalized as follows to ensure that the summation of powers will add up to the total available power in every iteration.

$$\left[P_{norm}\right]_i = \frac{\left[P_{new}\right]_i \times P_{Total}}{\sum_{i=1}^{L}\left[P_{new}\right]_i} \tag{3.25}$$

Table 5. Simulated Annealing (SA)

Algorithm 2	
1	$P_{current} = P_{initial}$
2	$D_{current} = D(P_{current})$
3	$D_{min} = D(P_{initial})$
4	$D_{old} = 10^{10}$
5	$iter = 0$
6	$\boldsymbol{while}\ (iter \leq iter_{Max})\boldsymbol{do}$
7	$P_{new} = choose\ random\ neighbor\ (P_{current})$
8	$P_{norm} = normalize\ (P_{new})$
9	$D_{new} = D(P_{norm})$
10	$\boldsymbol{if}\ (D_{new} < D_{min})\boldsymbol{then}$
11	$P_{best} = P_{norm}$
12	$D_{min} = D_{new}$
13	$\boldsymbol{end\ if}$
14	$\boldsymbol{if}(D_{new} < D_{current}) or\ (with\ certain\ probability)$
15	$P_{current} = P_{norm}$
16	$D_{current} = D_{new}$
17	$\boldsymbol{end\ if}$
18	$iter++$
19	$\boldsymbol{if}\left(remainder\binom{iter}{20} = 20\right)$
20	$\boldsymbol{if}\ (\lvert D_{new} - D_{old}\rvert < 0.1)$
21	$iter = iter_{max} + 1$
22	$\boldsymbol{end\ if}$
23	$D_{old} = D_{new}$
24	$\boldsymbol{end\ if}$
25	$\boldsymbol{end\ while}$

4.4. Channel Allocation and Power Adjustment

The purpose of the channel allocation block in Figure 22 is to further protect the important JPEG 2000 bits by transmitting them over sub-channels with higher quality. On the channel allocation block, sub-channels with better conditions are assigned to the important layers of JPEG2000 image. It can be inferred from Eq. (3.15) that by increasing h^{SP}, the imposed interference on the Primary user increases. Therefore, the ratio of h^{SS} to h^{SP}, can be an acceptable representation of the channel condition. This ratio is used as an index to compare the channels quality (higher ratio indicates better quality). We consider sub-channels with a ratio of h^{SS} to h^{SP} greater than a preset threshold, r_{th}, as "higher quality" vs. those with the ratio less than r_{th} as "lower quality" channels. During each signaling period, data from the most important layer of the JPEG2000 bitstream is sent on "higher quality" and data from the least important layer is sent on lower quality sub-channels. The detail of the algorithm is shown in Table 6.

Since the CSI is available at the time of transmission, after channel allocation for each OFDM symbol, power is adjusted such that both fading of the channel [33] and interference to the primary user limitation take into the account at the time of transmission.

Table 6. Channel allocation

Algorithm 3	
1	Select the threshold r_{th}
2	$LayerSize = [\ N_1, N_2, \dots, N_L]$
3	Set the counter $l_1\ for\ layer_1, l_2\ for\ layer_2, \dots, and\ l_L for\ layer_l$
4	$if\ ({h^{SS}}/{h^{SP}} > r_{th}\ )$
5	
6	Send data from $layer_1$ and $l_1 + +$ unless $l_1 > N_1$, send data from next layer, increase the corresponding counter by one and so on.
7	$end\ if$
8	
9	$if\ ({h^{SS}}/{h^{SP}} < r_{th}\ )$
10	Send data from $layer_L\ and\ l_L + + unless\ l_L > N_L$, send data from previous layer, increase the corresponding counter by one and so on.
11	$end\ if$

4.5. Simulation Results

In this section, the proposed method is used for transmission of Lenna, which is a grayscale image of size 512×512 and 8 bit/pixel. The Kakadu software is utilized as the JPEG2000 image coder. The performance of the method is studied further by investigating its impacts on several performance metrics (e.g., BER, PSNR). Futhermore, to assess the method's reliability and robustness, the same approach is applied on other images: Peppers, Cameraman, and Bridge.

The images are processed with one level of decomposition and are divided into 64×64 coding blocks and 128×128 precincts. The final images have 3 layers with the same size. 16 sub-carriers, one primary user, and one secondary user is considered. Table 3 shows the selected values for the model parameters based on the IEEE 802.11a standard [39].

The wireless channel is modeled as a frequency-selective channel with 2 multipaths. Each multipath is assumed to have Rayleigh-fading distribution with AWGN, and is independent of the other one. Here, the allocation period τ, is assumed to be the time needed for transmission of the entire image.

The average PSNR at the secondary user receiver for various SNRs is used to indicate the decoded image quality. Here, the performance of the system is analyzed by comparing the PSNR and BER profile of the received Lenna image transmitted through the listed scenarios in Table 7.

Table 7. Different applied scenarios

	Power Allocation	Channel Allocation
Scenario 1	EPA	N/A
Scenario 2	EPA	Based on the algorithm used in [6]
Scenario 3	UPA	N/A
Scenario 4	UPA	Based on the algorithm in Table 6

Figure 23 shows the average calculated PSNR value at various channel SNRs for four different resource allocation scenarios. As shown in Figure 23, Scenario 1, with EPA power allocation type, has the lowest performance among the considered scenarios. The performance in scenario 1 is increased when our previously proposed algorithm in [6] is utilized for channel allocation (i.e., scenario 2), to protect the important bits. However, the system performs better in scenario 3 by applying the UPA algorithm on the bit streams based on their impact on the received image quality. The performance is further improved in the 4th scenario by allocating the channels based on the proposed algorithm in Table 6. The observed improvements in the 3rd and 4th scenarios are significant even at low SNRs (SNR < 10 dB). As SNR goes beyond 20 dB there is no more improvement in the 3rd scenario's performance, since for higher SNRs the amount of power allocated to the important bits increases; hence without using an appropriate channel allocation, a huge interference for primary user may occur. Therefore, the allocated power is decreased to prevent intolerable interference to PU based on the

system constraint (see Eq.(4.1.d)), which results in performance reduction. This reduction can be negligible depending on the considered interference threshold, as will be seen in Figure 29. This issue is addressed in scenario 4 by using the proposed algorithm in Table 6 for channel allocation. Thus, it is observed that a proper channel allocation algorithm is a necessary condition for obtaining an enhanced performance, if UPA is used. It can also be expected that the average PSNR values of different methods converge to the same value at a high SNR, because at high SNR values the BER is very low, regardless of the power allocation algorithm. Note that one benefit of implementing UPA integrated with the proposed channel allocation algorithm is to reach to the highest possible PSNR at a lower SNR.

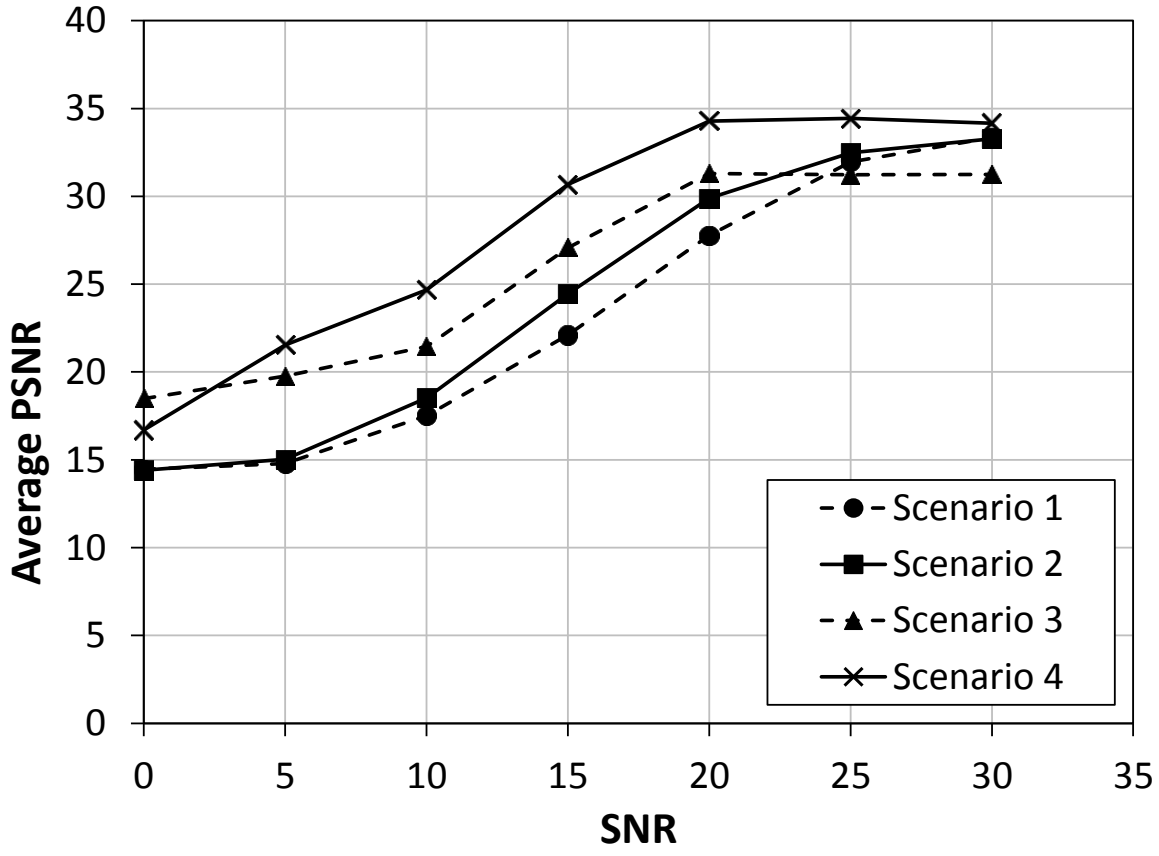

Figure 23. Average PSNR value versus SNR value for four different resource allocation scenarios

Figure 24 shows the BER performance of the received bit-streams of the Lenna image. BER represents the average probability of any bit being received with error,

regardless of its importance in the JPEG2000 bit-stream or the distortion of the received image, which PSNR is an indicator. Based on this definition, as it is plotted in Figure 24, there is no significant difference in the average BER of scenarios 1 and 2.

The proposed UPA algorithm protects important bits by allocating them higher powers (scenario 3), and the proposed channel allocation algorithm (scenario 4) allows transmission of higher importance bit streams through stronger sub-channels. By combining them together, we get lower protection of less important bits and consequently a higher BER at low SNR. However, the PSNR is significantly higher for scenarios 3 and 4. For SNR < 10 dB, the UPA algorithm has a preference to set the power of some less important coding passes to zero in order to minimize the distortion of the received image. This leads to a BER of 50% for bits with zero power and consequently a higher average BER over all bits. The number of coding passes with an assigned power of zero is gradually decreased as the SNR increases.

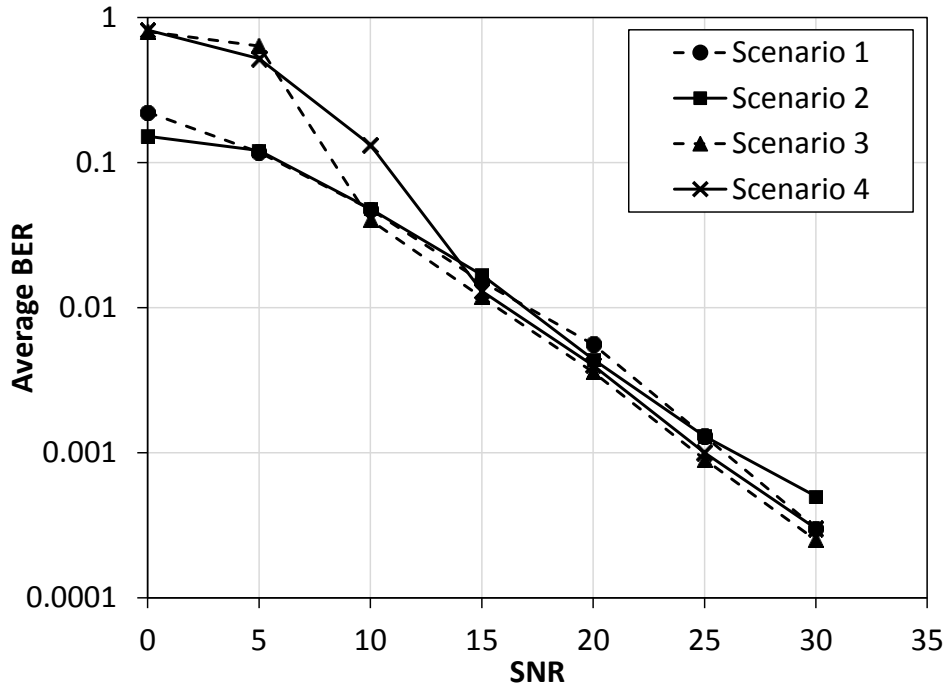

Figure 24.Average BER value versus SNR value for four different resource allocation scenarios

For better visual comparison, the transmitted Lenna image under different scenarios is shown in Figure 25. It can be seen that the visual quality of the received image is enhanced step by step applying scenarios 1 to 4 and the best image with more details is obtained by scenario 4, thanks to the UPA for power allocation and the proposed algorithm for channel allocation.

(a)

(b)

(c)

(d)

(e)

Figure 25. Visual comparison of "Lenna", transmitted at SNR=20 dB, (a) Original image (b) Scenario 1, PSNR =27.78 dB (c) Scenario 2, PSNR =29.89 dB (d) Scenario 3, PSNR =31.31 dB (e) Scenario 4, PSNR=34.29 dB

To assess the performance of our proposed method for other cases, the same procedure was applied to different images shown in Figure 26, Figure 27, and Figure 28. Similar result in quality improvement of receiving images were obtained.

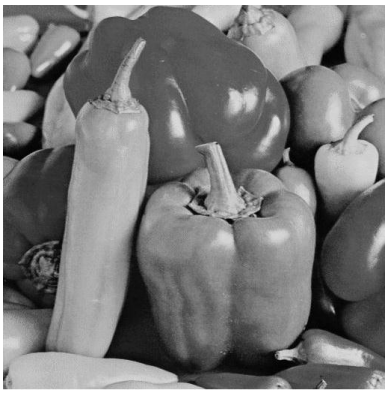

(a)

(b)

(c)

(d)

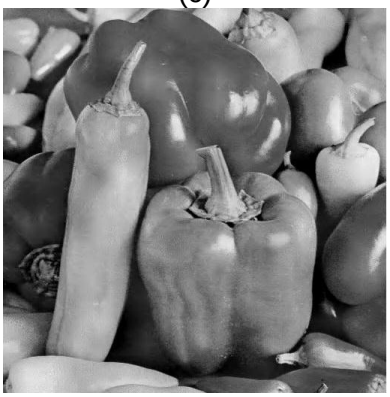

(e)

Figure 26. Visual comparison of "Peppers", transmitted at SNR=20 dB, (a) Original image (b) Scenario 1, PSNR =27.15 dB (c) Scenario 2, PSNR =29.12 dB (d) Scenario 3, PSNR =30.43 dB (e) Scenario 4, PSNR= 32.88 dB

(a)

(b)

(c)

(d)

(e)

Figure 27. Visual comparison of "Cameraman", transmitted at SNR=20 dB, (a) Original image (b) Scenario 1, PSNR =30.15 dB (c) Scenario 2, PSNR =30.63 dB (d) Scenario 3, PSNR = 31.68 dB (e) Scenario 4, PSNR= 36.34 dB

(a)

(b)

(c)

(d)

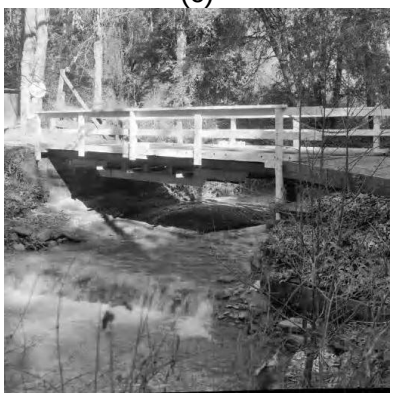

(e)

Figure 28. Visual comparison of "Bridge", transmitted at SNR=20 dB, (a) Original image (b) Scenario 1, PSNR =21.99 dB (c) Scenario 2, PSNR =23.02 dB (d) Scenario 3, PSNR = 23.54 dB (e) Scenario 4, PSNR= 27.13 dB

Figure 29, shows the effect of different interference thresholds, as determined by PU, on the PSNR of the received Lenna image at a channel SNR of *20* dB. It is expected as the threshold gets stricter the system performance drops. The first two scenarios show strong dependency of PSNR on the threshold, while by using UPA it is reduced. Moreover, it can be seen that scenario 4 performs the best at various thresholds, which makes it a good candidate for implementation in different communication networks.

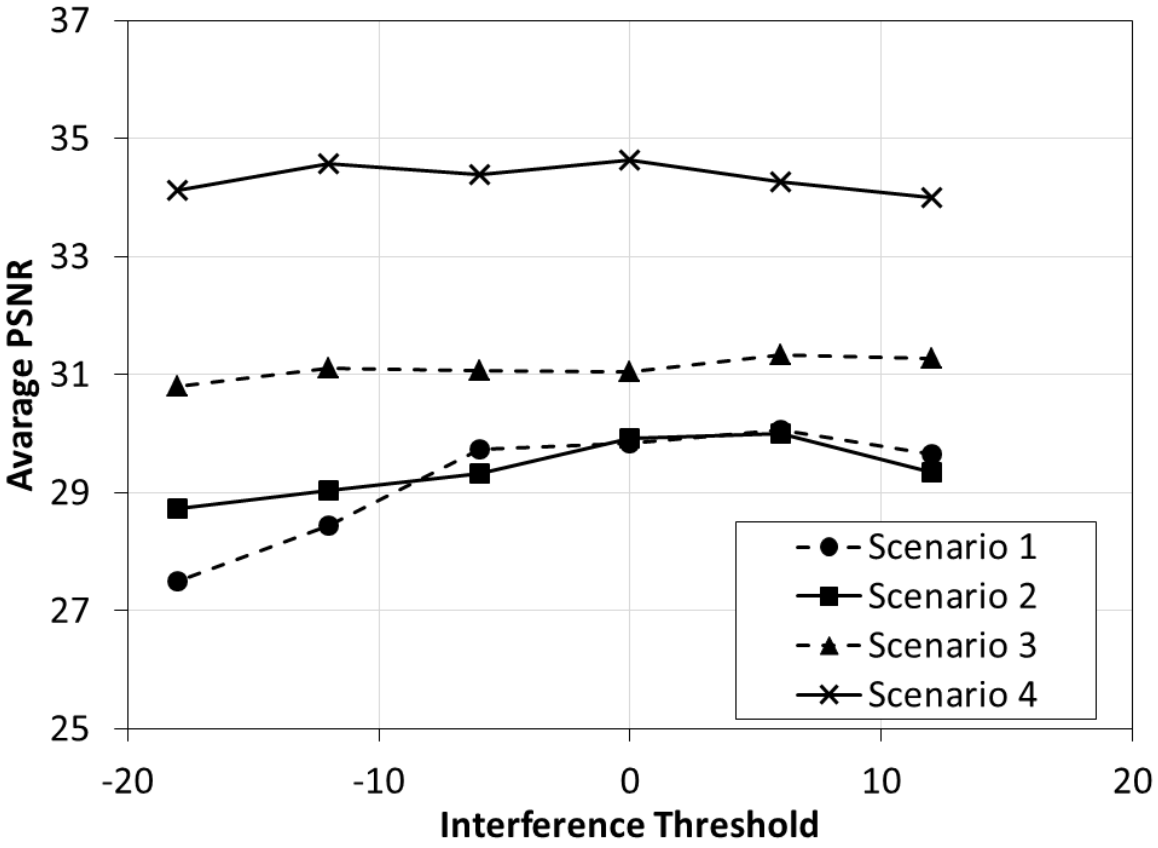

Figure 29.Average PSNR versus different interference threshold

4.6. Summary

In this chapter, resource allocation algorithm is applied to enhance the quality of transmitted JPEG2000 codec images over OFDM-based CR by considering the power and interference constraints. An optimization algorithm is used to allocate unequal power to the bits of the image bit - stream based on their impact on the image quality. The important bits in the lower layers are further protected by applying sub-channel allocation on top of UPA algorithm. The developed algorithm was observed to improve the secondary user's PSNR value without violating the primary user's interference limit. To assess the proposed approach, the algorithm was applied to image transmission according to IEEE 802.11a conditions. It was observed that this new technique can enhance the average PSNR significantly for multipath channels. Moreover, the BER performance of the received images is analyzed for different scenarios for power and channel allocations. It is noted that even though the unequal resource allocation scheme surpasses the EPA technique in PSNR performance for all SNR values, the BER curve of EPA technique shows lower values than the BER curve of the unequal resource allocation scheme for low SNRs (SNR < 10 dB). For visual assessment of the enhancements in transmitted quality of the the images with the proposed algorithm, four experiments with different images were carried out on Lenna, Peppers, Cameraman, and Bridge images.

Chapter 5.

Conclusion and future direction

5.1. Conclusion

Limited bandwidth is the major obstacle to delivering high quality multimedia services. In this thesis, we investigated the problem of transmitting multimedia content over cognitive radio networks, which is a newly emerged wireless communication paradigm that resolves the spectrum underutilization problem by being aware of the environment and having the ability to change its transmission parameters accordingly. We introduced a method to improve the received image quality in a cognitive radio system by taking advantage of the scalable bit-stream and application of unequal power allocations in two stages. The first stage optimizes the power allocated to the JPEG2000 bit-stream at the coding pass level to minimize the total received distortion. The second stage employs subcarrier allocation, adaptive modulation, and power adjustment to meet the interference requirements, based on channel conditions, and at the same time keeps the same throughput for the system. This strategy is shown to enhance the image quality, since important parts of the image will be transmitted more reliably.

In this study, we take advantage of OFDM for transmission of data in cognitive radio, to form the signal and use the spectrum holes more opportunistically. To maintain the overall transmit reliability, an adaptive modulation is adopted. Based on the number of available sub-channels to transmit the data, we mapped different modulation to keep a constant throughput. As the number of available sub-channels decrease due to primary user appearance or interference constraint, the modulation level increases.

5.2. Future Works

Throughout this thesis, we assumed a scenario with single primary and secondary user which transmitted JPEG2000 images over cognitive networks. The followings are the possible directions for the extension of this research:

- **Sensing frequency effect:**

  One possible direction to extend this work is to consider the sensing frequency of the bandwidth for checking the primary user's presence. This is an important factor in cognitive radio networks. An increase in this parameter will increase the pauses in transmission that can cause degradation in transmission quality.

- **Wireless channel model:**

  In this research, the fading channel distribution model was used for wireless channel modeling. However, other distribution models are also available such as: Rician and Nakagami. Therefore, it Is beneficial to study the performance of the resource allocation algorithms with various types of distribution models for the wireless channel.

- **Considering cooperative transmission scenarios:**

  One of the most common transmission methods in cognitive radio networks is cooperative transmission between different nodes in the network. Considering this method, if the direct channel between transmitter and receiver has poor conditions, the transmitter can use other nodes to send the data in order to gain a better quality in receiver side.

References

[1] S. Verdú, “Wireless bandwidth in the making,” *IEEE Commun. Mag.*, vol. 38, no. 7, pp. 53–58, 2000.

[2] “Spectrum Policy Task Force Report FCC 03-289,” 2003.

[3] I. F. Akyildiz, W.-Y. Lee, M. C. Vuran, and S. Mohanty, “NeXt generation/dynamic spectrum access/cognitive radio wireless networks: A survey,” *Comput. Networks*, vol. 50, no. 13, pp. 2127–2159, 2006.

[4] T. Weiss and F. K. Jondral, “Spectrum pooling: An innovative strategy for the enhancement of spectrum efficiency,” *IEEE Commun. Mag.*, vol. 42, no. 3, pp. 8–14, 2004.

[5] W. Jian, Y. Longxiang, and L. Xu, “Subcarrier and Power Allocation in OFDM Based Cognitive Radio Systems,” *2011 Fourth Int. Conf. Intell. Comput. Technol. Autom.*, vol. 2, pp. 728–731, 2011.

[6] G. Javadi, A. Hajshirmohammadi, and J. Liang, “JPEG2000 Image Transmission Over OFDM-Based Cognitive Radio Network,” in *Computing and Communication (IEMCON), 2015 International Conference and Workshop)*, 2015, pp. 1–6.

[7] Q. Zhao, L. Tong, A. Swami, and Y. Chen, “Decentralized cognitive MAC for opportunistic spectrum access in ad hoc networks: A POMDP framework,” *IEEE J. Sel. Areas Commun.*, vol. 25, no. 3, pp. 589–599, 2007.

[8] G. Ganesan and Y. Li, “Cooperative spectrum sensing in cognitive radio, part I: Two user networks,” *IEEE Trans. Wirel. Commun.*, vol. 6, no. 6, pp. 2204–2212, 2007.

[9] G. Ganesan and Y. (Geoffrey) Li, “Cooperative spectrum sensing in cognitive radio, part II: Multiuser networks,” *Ieee Trans. Wirel. Commun.*, vol. 6, no. 6, pp. 2214–2222, 2007.

[10] A. Ahmed, L. M. Boulahia, and D. Gati, “Enabling vertical handover decisions in heterogeneous wireless networks: A state-of-the-art and a classification,” *IEEE Commun. Surv. Tutorials*, vol. 16, no. 2, pp. 776–811, 2014.

[11] S. Haykin, “Cognitive radio: Brain-empowered wireless communications,” *IEEE J. Sel. Areas Commun.*, vol. 23, no. 2, pp. 201–220, 2005.

[12] Q. Zhao and B. M. Sadler, “A Survey of Dynamic Spectrum Access,” *IEEE Signal Process. Mag.*, vol. 24, no. 3, pp. 79–89, 2007.

[13] C. G. K. (Korea U. Yong Soo Cho (Chung-Ang University), Jaekwon Kim (Chung-Ang University), Won Young Yang (Chung-Ang University), *MIMO-OFDM Wireless Communications with MATLAB*, vol. 53, no. 9. John Wiley & Sons (Asia) Pte Ltd, 2013.

[14] J. E. Ingvaldsen, O. Ozgobek, and J. A. Gulla, “Context-aware user-driven news recommendation,” in *CEUR Workshop Proceedings*, 2015, vol. 1542, pp. 33–36.

[15] A. K. L. Gray and B. Andrea, “The JPEG2000 Standard,” pp. 1–23.

[16] A. Skodras, C. Christopoulos, and T. Ebrahimi, “The JPEG 2000 still image compression standard,” *IEEE Signal Process. Mag.*, vol. 18, no. 5, pp. 36–58, 2001.

[17] D. Taubman and M. Marcellin, *JPEG2000 Image Compression, Fundamentals, Standards, and Practice*. Norwell, Massachusetts: Kluwer Academic Publishers, 2002.

[18] D. T. Ngo, C. Tellambura, and H. H. Nguyen, “Resource allocation for OFDMA-based cognitive radio multicast networks with primary user activity consideration,” *IEEE Trans. Veh. Technol.*, vol. 59, no. 4, pp. 1668–1679, 2010.

[19] M. Dashti, K. Navaie, and P. Azmi, “Radio resource allocation for orthogonal frequency division multiple access-based underlay cognitive radio networks utilising weighted ergodic rates,” *IET Commun.*, vol. 6, no. 16, pp. 2543–2552, 2012.

[20] Jiho Jang and Kwang-Bok Lee, “Transmit power adaptation for multiuser OFDM systems,” *IEEE J. Sel. Areas Commun.*, vol. 21, no. 2, pp. 171–178, 2003.

[21] H. Zhu, “Radio resource allocation for OFDMA systems in high speed environments,” *IEEE J. Sel. Areas Commun.*, vol. 30, no. 4, pp. 748–759, 2012.

[22] S. Li, T. H. Luan, and X. Shen, “Channel Allocation for Smooth Video Delivery over Cognitive Radio Networks,” *2010 IEEE Glob. Telecommun. Conf. GLOBECOM 2010*, pp. 1–5, 2010.

[23] R. Yao, Y. Liu, J. Liu, P. Zhao, and S. Ci, “Utility-based H.264/SVC video streaming over multi-channel cognitive radio networks,” *IEEE Trans. Multimed.*, vol. 17, no. 3, pp. 434–449, 2015.

[24] H. Saki and M. Shikh-Bahaei, “Cross-layer resource allocation for video streaming over OFDMA cognitive radio networks,” *IEEE Trans. Multimed.*, vol. 17, no. 3, pp. 333–345, 2015.

[25] M. L. Tham, C. O. Chow, M. Iwahashi, and H. Ishii, “BER-driven resource allocation for scalable bitstreams over OFDMA networks,” *IEEE Trans. Veh. Technol.*, vol. 63, no. 6, pp. 2755–2768, 2014.

[26] B. Guan and Y. He, “Optimal Resource Allocation for Multi-layered Video Streaming over Multi-channel Cognitive Radio Networks,” *Trust. Secur. Priv. Comput. Commun. (TrustCom), 2012 IEEE 11th Int. Conf.*, pp. 1525–1528, 2012.

[27] F. Hou, Z. Chen, J. Huang, Z. Li, and A. K. Katsaggelos, “Multimedia multicast service provisioning in cognitive radio networks,” in *2013 9th International Wireless Communications and Mobile Computing Conference, IWCMC 2013*, 2013, pp. 1175–1180.

[28] H. A. Karim, H. Mohamad, N. Ramli, and A. Sali, “Scalable Video Streaming over Overlay / Underlay Cognitive Radio Network,” in *International Symposium on Communication and Information Technologies*, 2012, pp. 668–672.

[29] J. Huang, Z. Zhang, H. Wang, and H. Liu, “Video transmission over Cognitive Radio networks,” *2011 IEEE GLOBECOM Work. (GC Wkshps)*, pp. 6–11, 2011.

[30] H. Shiang and M. Van Der Schaar, “Dynamic Channel Selection for Multi-User Video Streaming Over,” in *15th IEEE International Conference on Image Processing*, 2008, pp. 2316–2319.

[31] X. L. Huang, G. Wang, F. Hu, and S. Kumar, “The impact of spectrum sensing frequency and packet-loading scheme on multimedia transmission over cognitive radio networks,” *IEEE Trans. Multimed.*, vol. 13, no. 4, pp. 748–761, 2011.

[32] C. Ye, G. Ozcan, M. C. Gursoy, and S. Velipasalar, “Image and Video Transmission in Cognitive Radio Systems under Sensing Uncertainty,” in *IEEE*

Wireless Communications and Networking Conference, 2015, pp. 417–422.

[33] M. Shayegannia, A. Hajshirmohammadi, S. Muhaidat, and M. Torki, “Transmission of JPEG2000 images over frequency-selective channels with unequal power allocation,” *IET Image Process.*, vol. 7, no. 1, pp. 33–41, 2013.

[34] B. Banister, B. Belzer, and T. R. Fischer, “Robust Image Transmission Using JPEG2000,” *IEEE Signal Process. Lett.*, vol. 9, no. 4, pp. 117–119, 2002.

[35] S. S. Arsalan, P. C. Cosman, and L. B. Milstein, “Progressive Image Transmission,” *IEEE Trans. Veh. Technol.*, vol. 60, no. 9, pp. 4299–4313, 2011.

[36] J. G. Proakis, *Digital Communication*. Boston: McGraw-Hill, 2000.

[37] A. H. Sayed, *Adaptive Filters*. Hoboken, New jersey: John Wiley & Sons Inc, 2008.

[38] T. Weiss, J. Hillenbrand, A. Krohn, and F. K. Jondral, “Mutual interference in OFDM-based spectrum pooling systems,” *2004 IEEE 59th Veh. Technol. Conf.*, vol. 4, pp. 1873–1877, 2004.

[39] L. S. Committee, “Part 11: Wireless LAN medium access control (MAC) and physical layer (PHY) specifications,” *IEEE-SA Stand. Board*, vol. 1999, no. June, 2003.

[40] I. Moccagatta, S. Soudagar, J. Liang, and H. Chen, “Error-Resilient Coding in JPEG-2000 and MPEG-4,” *IEEE J. Sel. Areas Commun.*, vol. 18, no. 6, pp. 899–914, 2000.

[41] M. Torki and A. Hajshirmohammadi, “Unequal Power Allocation for Transmission of JPEG2000 Images over Wireless Channels,” *Commun. Soc.*, pp. 1–6, 2009.